(12) INTERNATIONAL APPLICATION PUBLISHED UNDER THE PATENT COOPERATION TREATY (PCT)

(19) World Intellectual Property Organization
International Bureau

(43) International Publication Date
23 January 2014 (23.01.2014)

WIPO | PCT

(10) International Publication Number
WO 2014/012182 A1

(51) International Patent Classification:
G01T 1/164 (2006.01) *G01T 1/169* (2006.01)

(21) International Application Number:
PCT/CA2013/050556

(22) International Filing Date:
18 July 2013 (18.07.2013)

(25) Filing Language: English

(26) Publication Language: English

(30) Priority Data:
61/673,343 19 July 2012 (19.07.2012) US

(71) Applicant: **UNIVERSITY OF SASKATCHEWAN** [CA/CA]; Industry Liaison Office, Suite 501, 121 Research Drive, Saskatoon, Saskatchewan S7N 1K2 (CA).

(72) Inventor: **RANGACHARYULU, Chilakamarri**; 902 Temperance Street, Saskatoon, Saskatchewan S7N 0N4 (CA).

(74) Agent: **BERESKIN & PARR LLP/S.E.N.C.R.L., S.R.L.**; 40 King Street West, Suite 4000, Toronto, Ontario M5H 3Y2 (CA).

(81) Designated States *(unless otherwise indicated, for every kind of national protection available)*: AE, AG, AL, AM, AO, AT, AU, AZ, BA, BB, BG, BH, BN, BR, BW, BY, BZ, CA, CH, CL, CN, CO, CR, CU, CZ, DE, DK, DM, DO, DZ, EC, EE, EG, ES, FI, GB, GD, GE, GH, GM, GT, HN, HR, HU, ID, IL, IN, IS, JP, KE, KG, KN, KP, KR, KZ, LA, LC, LK, LR, LS, LT, LU, LY, MA, MD, ME, MG, MK, MN, MW, MX, MY, MZ, NA, NG, NI, NO, NZ, OM, PA, PE, PG, PH, PL, PT, QA, RO, RS, RU, RW, SC, SD, SE, SG, SK, SL, SM, ST, SV, SY, TH, TJ, TM, TN, TR, TT, TZ, UA, UG, US, UZ, VC, VN, ZA, ZM, ZW.

(84) Designated States *(unless otherwise indicated, for every kind of regional protection available)*: ARIPO (BW, GH, GM, KE, LR, LS, MW, MZ, NA, RW, SD, SL, SZ, TZ, UG, ZM, ZW), Eurasian (AM, AZ, BY, KG, KZ, RU, TJ, TM), European (AL, AT, BE, BG, CH, CY, CZ, DE, DK, EE, ES, FI, FR, GB, GR, HR, HU, IE, IS, IT, LT, LU, LV, MC, MK, MT, NL, NO, PL, PT, RO, RS, SE, SI, SK, SM, TR), OAPI (BF, BJ, CF, CG, CI, CM, GA, GN, GQ, GW, KM, ML, MR, NE, SN, TD, TG).

Published:

— *with international search report (Art. 21(3))*

(54) **Title**: PET AND SPECT MULTI PHOTON IMAGING WITH SINGLE RADIOACTIVE ISOTOPES

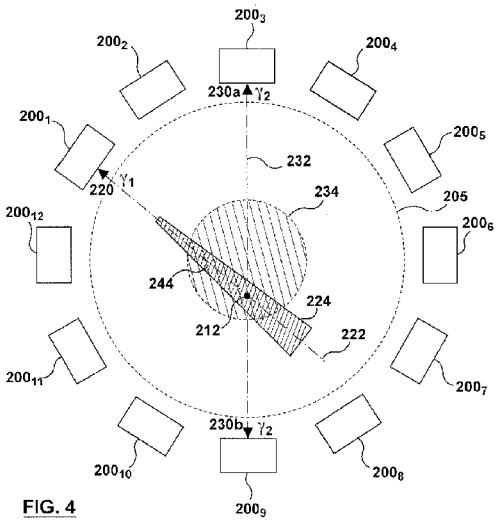

FIG. 4

(57) **Abstract**: Systems and methods for determining an approximate location of a radionuclide at a time of its radioactive decay are described. In one embodiment, the method comprises introducing into a target region a radionuclide that, at the time of its radioactive decay, emits a positron and a primary photon, detecting the primary photon at a first one of a plurality of photon detectors and detecting at least one secondary photon emitted from an annihilation of the position at least a second one of the plurality of photon detectors, and determining the approximate location of the radionuclide at the time of its radioactive decay based on a location of the first one of the plurality of photon detectors, a location of the second one of the plurality of photon detectors, and a presumed common point of origin of the detected primary photon and the detected at least one secondary photon.

WO 2014/012182 A1

TITLE: PET AND SPECT MULTI PHOTON IMAGING WITH SINGLE RADIOACTIVE ISOTOPES

PRIOR APPLICATION

[0001] This application claims the benefit of United States Provisional Patent Application No. 61/673,343 filed on July 19, 2012 entitled "PET AND SPECT MULTI PHOTON IMAGING WITH SINGLE RADIOACTIVE ISOTOPES", which is incorporated by reference herein in its entirety

FIELD

[0002] Embodiments disclosed herein relate generally to systems and methods for nuclear imaging, including Positron Emission Tomography and Single-Photon Emission Computed Tomography.

BACKGROUND

[0003] Positron Emission Tomography (PET) employs a radioisotope that emits a positron (antiparticle of electron) when it undergoes radioactive decay. The positron subsequently annihilates with an electron in the surroundings, typically resulting in two relatively high energy photons (gamma rays) travelling along a straight line in opposite directions (approximately 180 degrees apart). These photons can be detected using gamma detectors, and their line of flight can be reconstructed and used to estimate the location of the positron annihilation event.

[0004] Single Photon Emission Computed Tomography (SPECT) is also based on the detection of photons. However, unlike in PET, the radioisotopes typically used in SPECT emit a photon directly during radioactive decay. As the origin of the photon emission is based on a single photon, the gamma cameras are typically unable to determine depth information. Instead, a number of two-dimensional images are captured from a number of different angles, and a computer is used to generate a tomographic reconstruction of these multiple 2-D images (or projections).

BRIEF DESCRIPTION OF THE DRAWINGS

[0005] For a better understanding of the example embodiments described herein and to show more clearly how they may be carried into effect, reference will now be made, by way of example, to the accompanying drawings in which:

[0006] FIG. 1 is a plot of fractional energy changes for 511 keV PET photons and 142 keV ^{99m}Tc SPECT photons as a function of angle;

[0007] FIG. 2 is a schematic representation of the detection of a photon emitted as a result of radioactive decay of a radionuclide;

[0008] FIG. 3 is a schematic representation of the detection of photons emitted as a result of positron annihilation;

[0009] FIG. 4 is a schematic representation of the detection of a photon emitted as a result of radioactive decay of a positron emitting radionuclide and photons emitted as a result of positron annihilation according to one embodiment;

[0010] FIG. 5 is a schematic representation of the detection of photons emitted as a result of radioactive decay of a radionuclide according to one embodiment;

[0011] FIG. 6 is a schematic block diagram of a detector system according to one embodiment;

[0012] FIG. 7 shows the neutron cross section (a measure of production rate) for ^{123}Xe plotted against proton energy; and

[0013] FIG. 8 shows the neutron cross section (a measure of production rate) for ^{73}Se plotted against proton energy.

DETAILED DESCRIPTION

[0014] Positron Emission Tomography (PET) and Single Photon Emission Computed Tomography (SPECT) are imaging techniques used in medical research and diagnosis. Positron Emission Tomography employs a radioisotope which emits a positron (the antiparticle of electron). The positron subsequently annihilates with an electron in the surroundings, resulting in two 511 keV photons (gamma rays) travelling along an approximately straight line in opposite directions (i.e. 180 degrees apart). The PET technique registers the two photons entering the detectors to reconstruct the line of flight of the photons.

[0015] In more recent PET machines, the origin of the photons (e.g. the location of the positron annihilation) can be estimated to about a centimeter precision by employing the time of flight information of the detected photons. For example, if

two 511 keV photons are detected at two detectors within a predetermined time interval, they are assumed to have originated from the same annihilation event; this annihilation event is assumed to have taken place along a reconstructed line of flight of the photons (e.g. a line between the two detectors). Also, the annihilation event can be estimated to have taken place closer to the detector that detected the first of the two detected photons, this estimated distance being proportional to the elapsed time between the detection of the two photons.

[0016] Also, PET assumes that the point of photon emission is same as the location where the radioisotope decays – e.g. the location of the emission of the positron. However, positrons emitted during radioactive decay are moving at high speeds, almost 30-70% of speed of light. This would mean that in many cases, the positron annihilation point is not the same as the location where the positron was "born" (i.e. emitted). Thus, a location of a radioisotope determined by a PET scan may not represent the precise location of the radioisotope from which it is emitted. From Monte Carlo simulations, it has been estimated that positrons could migrate as much as a few millimeters before annihilation [See e.g. J. Cal- González, J.L. Herriaz, S. España, M. Desco, J.J. Vaquero, J. M. Udías, Proceedings of IEEE conference on Nuclear Science and Medical Imaging (2009) p.2788-2791].

[0017] While PET utilizes pairs of photons emitted from positron-electron annihilation events, Single Photon Emission Computed Tomography (SPECT) makes use of one photon emitted directly from gamma-emitting radionuclides. While a SPECT photon originates at the decay vertex of the isotope - i.e. there is no material difference in the location of the photon emission and the location of the radioisotope at the time of this emission – the one photon imaging does not provide depth information.

[0018] Instead, similar to X-ray computed tomography techniques (e.g. Computed Tomography (CT) or Computed Axial Tomography (CAT)), multiple two-dimensional images of photon emission – each taken at a different angle with respect to the target sample being scanned – are post-processed in order to create a three-dimensional volumetric image (also referred to as a tomographic reconstruction, or simply a tomogram) of the target sample.

[0019] Common radionuclides used for nuclear imaging include ^{11}C, ^{13}N and ^{18}F for PET and ^{99m}Tc, ^{67}Ga, ^{111}In and ^{123}I for SPECT. It is also common to incorporate the radionuclide (also referred to as a radioactive tracer) into a larger active molecule localized in the body. An example that is frequently used for PET imaging is fluorodeoxyglucose (FDG). FDG is a biologically active glucose analog and it is commonly used for medical diagnosis such as detection and localization of tumors.

[0020] Even though modern PET and SPECT technology allows three dimensional imaging of the body at a reasonable resolution, there are some known drawbacks. In addition to artifacts that are common to all CT systems (e.g. artifacts associated with the back-projection process and patient-induced artifacts), both PET and SPECT have their own limitations that can result in ambiguities and misdiagnoses. These limitations include photon absorption and scattering.

[0021] To help correct for absorption effects, physics suggests that dual energy imaging – which employs photons of two distinct energies – may be useful. For this purpose, PET/CT and SPECT/CT imaging are commonly employed.

[0022] Attenuation correction must be made in both PET and SPECT and the process for correction is different for each. For instance, attenuation in PET is different from attenuation in SPECT because PET requires both photons from an annihilation event to reach the detectors for a coincident event to be registered. As a result, the probability that the two PET photons emitted from a single annihilation event will be attenuated (i.e. a product of the attenuation probability for each photon, each attenuation probability being less than one) is less than the probability that one single photon emitted during radioactive decay (e.g. in SPECT) will be attenuated.

[0023] Also, the attenuation is a sensitive function of photon energies. SPECT photons are usually of much lower energy (<200 keV) while the PET photons are of 511 keV. The lower energy SPECT photons are more likely to be absorbed rather than scattered, resulting in a loss of intensity or information rather than a misidentification.

[0024] Regarding photon scattering, the emitted photons can be scattered (i.e. deflected) on their way to the gamma detectors. This can result in a misidentification

of their point of origin. While collimators are typically used to help reduce image artifacts, their use may lower the contrast resolution of the detector due to a decreased signal-to-noise (SNR) ratio. Also, while large angle scattering of photons may be discarded as the photon energy will be quite different from the expected PET/SPECT photon energies, the finite resolution of detectors may admit scatters as large as 30 degrees for PET detectors, and even much larger angles for SPECT detectors.

[0025] Figure 1 shows fractional energy changes for 511 keV PET photons and 142 keV 99^{m}Tc SPECT photons as a function of angle.

[0026] This calculation is based on the standard Compton Scattering formula:

$$E_{\gamma}(Scatter) = \frac{E_{\gamma}}{1+1.957E_{\gamma}(1-\cos\theta)} \qquad (1)$$

wherein E_γ is the photon energy expressed in MeV units, θ is the angle at which photon is scattered and E_γ (scatter) is the energy of scattered photons. Figure 1 is a plot of fractional energy loss in the photon due to scattering, i.e.

$$fraction = \frac{E_{\gamma} - E_{\gamma}(scatter)}{E_{\gamma}} \qquad (2)$$

[0027] For conventional scintillation detectors with resolutions of 5-10%, it becomes apparent that scattering effects cannot be estimated from energy measurements for angles less than about 30 degrees, which may contribute to misidentification of the emission point. Clearly, detectors with a relatively higher resolution fare better in this regard.

[0028] Regarding photon absorption, photons can be absorbed (e.g. lost) between emission and the detectors. This loss of information can set a limit on the achievable contrast. Also, it is often unclear if the photon is absorbed in the human body or somewhere else on its way before its gets into the sensitive volume of the detector.

[0029] It was realized early on that neither a PET nor a SPECT technique, by itself, provides unambiguous images due to several artifacts, such as absorption and scattering of photons in the sample and surroundings. Several techniques such as

PET/CT and SPECT/CT (and/or other combinations with Magnetic Resonance Imaging (MRI), etc.) are being developed with mixed results. Dual energy imaging with multiple sources (i.e. multiple radioisotopes) is also being considered as a possible option. While these methods may improve image qualities, uncorrelated decays of two or more radioactive sources of different half-lives would:

a) cause random emissions from the sample with each isotope decaying at different locations and times in patient's body with no direct correlation between source points;

b) necessitate administering higher doses of radiation to patients (as they would need to have two separate radioisotopes injected into their bodies); and,

c) increase imaging times (as patients would need to undergo a separate scan for each radioisotope).

[0030] Also, if the half-lives of the two or more radioisotopes are significantly different, the result could effectively be a single isotope imaging of either the PET or SPECT variety, unless one administers a relatively high dose of the radioisotope (PET or SPECT isotope) with the shorter half-life to achieve an effective combined imaging over the life of the radioisotope with the longer half-life, and even then it is likely that the relative intensities of the two radioisotopes will result in imaging based on one of the two energies being dominant (e.g. either the PET or SPECT variety). Providing two separate isotopes with comparable half-lives, that emit photons of comparable intensities over the entire imaging time, and that can be incorporated into tracer compounds having a similar biological response such that the isotopes undergo radioactive decay at nearly the same location inside a patient is impractical (if not impossible).

[0031] In case of SPECT/CT, an additional disadvantage is that the SPECT photon (typically having an energy of about 140 to about 200 keV) and CT X-ray photons (typically having an energy of about 100 to about 120 keV) may not constitute distinct enough energies to provide significant attenuation information.

[0032] In the literature, suggestions and some assays were made with two isotopes or even three isotopes to achieve multi-energy imaging [Y. Du and E.C. Frey, Proceedings of IEEE conference on Nuclear Science (2007), p. 4213-4216].

This technique, while acquiring data simultaneously, is a collection of data of random emissions of photons without temporal or spatial coincidences. Also, the energies of photons are close and cross talk between them brings its own artifacts and aberrations.

[0033] Each of these methods may have the following disadvantages:

1) They typically require additional infrastructure for imaging in both hardware and software;

2) They produce, in effect, two uncorrelated images produced by unrelated photon interactions;

3) The imaging times may become longer;

4) They may require the production of two or more different isotopes, likely by different production mechanisms and/or by different production and chemical processing protocols; and

5) Patients may be administered higher radiation doses (due to the exposure to two or more separate radiation sources).

[0034] Embodiments of the present invention provide an improved method for determining an approximate location of a radionuclide at a time of its radioactive decay. The method involves the use of a single radioisotope consisting essentially of radionuclides that, at the time of their radioactive decay, emit both a positron and a primary photon.

[0035] By using a radioisotope that emits positrons accompanied by photons emitted from a daughter product of the decay path – the positron and a primary photon being emitted within a relatively small time interval (e.g. a separation of less than a picosecond) – a result is a method of dual energy imaging that may be highly localized in both space and time. That is, during this time interval, the positron-emitting source typically moves less than a micron, while the positron itself may migrate up to a few millimeters from the location of the emission of the primary photon before annihilation. Therefore, the positron annihilation photons and the primary photon are both temporally and spatially correlated.

[0036] By detecting temporally and spatially correlated emissions of multiple photons having different energies, one may be able to draw more definitive conclusions regarding a location of the radionuclide at the time of its decay. As the emission point may be localized with greater spatial resolution, this may lead to 3-D imaging that is more accurate – and in some cases may be much more accurate – than, for example, single photon X-ray imaging, single photon SPECT imaging, or two photon PET imaging.

[0037] By using a single radioisotope, embodiments described herein may reduce the amount of radiation administered to a patient during medical imaging. For example, data that would ordinarily require both a PET and separate SPECT scan to be conducted (which would normally require two separate radioisotopes to be administered) may be acquired using only a single radioisotope. Also, data acquisition time may be reduced (as only one scan – not two –is required), which may make the process less strenuous to the patient. The technical staff time may also be decreased.

[0038] Also, the use of two or more separate radioisotopes (i.e. one for PET and another for SPECT), in addition to requiring injections of two isotopes, may entail inefficient and excessive dosages of isotopes to be administered, as the two isotopes will likely not have identical half-lives. Also, the two sets of measurements on patients would typically result in separate data sets (one for PET and another for SPECT) which are uncorrelated with each other. That is, the intensities and half-lives of the two sources are uncorrelated, and there is no temporal or locational correlation between separate emission events. By detecting temporally and spatially correlated emission data, the accuracy or precision or both of the determined locations or decay events may be improved.

[0039] Also, by using a single radioisotope, the isotope production method as well as other chemical processing required to prepare an isotope sample to be administered to a patient may be simplified. Use of a single radioisotope will typically involve only one production method and one chemical processing system, rather than two separate production channels and chemical treatments that would typically be needed to prepare and administer two separate isotopes.

[0040] In some embodiments, our methods may be implemented using the latest generation of PET machines without significant changes to the hardware. Current generation PET machines typically operate using "list-mode" data collection, in which a time-indexed list of photon detections is generated. For a number of radionuclide decay events, it is possible that not all photons of interest from that decay event will be detected. For example, not all emitted photons may reach a photon detector, or some photons may 'hit' a detector but go unrecorded due to the detectors having less than 100% detection efficiency, or both. Using list-mode may provide flexibility to classify and/or group detection events separately as detection events where three photons are detected (the primary photon and a pair of positron annihilation photons) and as detection events where only two or one of the three photons emitted during a radioactive decay of a radionuclide are detected. By selectively ignoring certain detected photons (e.g. ignoring photons having an expected energy), data validity can be cross checked and several artifacts can be examined. Using a technique referred to as "software cuts", multiple images – each image being generated based on specific logic conditions – may be created to critically evaluate physical and geometrical artifacts to facilitate false-negative and false-positive diagnostics.

[0041] In one broad aspect, there is provided a method of determining an approximate location of a radionuclide at a time of radioactive decay of the radionuclide, the method comprising: providing a plurality of photon detectors directed towards a target region, introducing into the target region the radionuclide that, at the time of its radioactive decay, emits a positron and a primary photon, detecting the primary photon at a first one of the plurality of photon detectors and detecting at least one secondary photon emitted from an annihilation of the positron at at least a second one of the plurality of photon detectors, and determining the approximate location of the radionuclide at the time of its radioactive decay based on a location of the first one of the plurality of photon detectors, a location of the second one of the plurality of photon detectors, and a presumed common point of origin of the detected primary photon and the detected at least one secondary photon.

[0042] In some embodiments, the primary photon is emitted from a daughter product of the radionuclide following the emission of the positron.

[0043] In some embodiments, the plurality of photon detectors is capable of characterizing a detected photon as either primary or secondary.

[0044] In some embodiments, the primary photon has a primary expected energy, the at least one secondary photon has a secondary expected energy, and the characterizing is based on a comparison of a detected energy of the detected photon and at least one of the primary and secondary expected energies.

[0045] In some embodiments, the determining is further based on a time of detection of the primary photon and a time of detection of each of the at least one secondary photon.

[0046] In some embodiments, the detecting at least one secondary photon comprises detecting two secondary photons.

[0047] In some embodiments, the approximate location of the radionuclide at the time of its radioactive decay is determined based on a selected two of the three detected photons.

[0048] In some embodiments, the approximate location of the radionuclide at the time of its radioactive decay is determined based on a selected one of the three detected photons.

[0049] In some embodiments, the detecting of the primary photon and the at least one secondary photon is performed during a predetermined time interval.

[0050] In some embodiments, the plurality of photon detectors comprises a ring of photon detectors disposed about the target region.

[0051] In some embodiments, the introducing comprises introducing a molecule or compound tagged with a plurality of radionuclides into the target region.

[0052] In some embodiments, the method further comprises repeating the detecting over a plurality of predetermined time intervals, and for substantially each predetermined time interval in the plurality of predetermined time intervals during which one of the plurality of radionuclides undergoes radioactive decay, determining the approximate location of that radionuclide at the time of its radioactive decay based on a presumed common point of origin of photons detected during that predetermined time interval.

[0053] In some embodiments, the method further comprises determining a volumetric reconstruction of a concentration of the plurality of radionuclides within the object based on a statistical reconstruction of the determined approximate locations of substantially each of the plurality of radionuclides.

[0054] In some embodiments, the radionuclide is 123Xe, 73Se, 75Br, 174Ta, 99Rh, or 184Ir. In some embodiments,. the method of claim 14, wherein the radionuclide is 123Xe. In some embodiments, the radionuclide is 73Se.

[0055] In another broad aspect, there is provided a system for determining an approximate location of a radionuclide that, at the time of its radioactive decay, emits a positron and a primary photon, the system comprising: a plurality of photon detectors directed towards a target region, the plurality of photon detectors capable of detecting the primary photon at a first one of the plurality of photon detectors and detecting at least one secondary photon emitted from an interaction of the positron and an electron at least a second one of the plurality of photon detectors, and a computing device capable of determining the approximate location of the radionuclide at the time of its radioactive decay based on a location of the first one of the plurality of photon detectors, a location of the second one of the plurality of photon detectors, and a presumed common point of origin of the detected primary photon and the detected at least one secondary photon.

[0056] In another broad aspect, there is provided a method of localizing a radioisotope within a target region at a time of radioactive decay of the radioisotope, the method comprising: providing at least one photon detector directed towards the target region, introducing the radioisotope into the target region, the radioisotope comprising a radioisotope that, at the time of radioactive decay, emits a positron and at least one primary photon, detecting the at least one primary photon and at least one secondary photon emitted from an interaction of the positron and an electron using the at least one photon detector, and localizing the radioisotope based on the detected at least one primary photon and the detected at least one secondary photon.

[0057] These and other aspects and features of various embodiments will be described in greater detail below. Embodiments of the present application provide methods for determining an approximate location of a radionuclide that, at a time of

its radioactive decay, emits both a primary photon and a positron. In order to aid in the understanding of the general methods, specific embodiments are described below as an example of the general method; it is to be understood that alternate embodiments are feasible. For example, different embodiments may, in variant implementations, be associated with radioisotopes not specifically mentioned, or using other types of photon detection equipment.

[0058] Figure 2 is an illustrative schematic example of single photon imaging in which a number of photon detectors 200 are directed towards a target region 205 that contains a radionuclide 210. As this radionuclide 210 undergoes radioactive decay, a primary photon 220 having an energy γ_1 (referred to herein as a primary energy) is emitted and subsequently detected at detector 200_1. Based on the location of photon detector 200_1 at which this primary photon 220 is detected, an approximate location of the radionuclide at the time of its radioactive decay (i.e. the source of the primary photon emission) can be estimated as being somewhere along a line of flight 222. In practice, based on the acceptance of photon detectors 200 (i.e. the angle of view of the detectors, which is typically a function of the size and geometry of the individual detector elements including, for example, one or more collimators), the approximate location of the photon emission event may be estimated as being within the three dimensional region 224, which may be a substantially cylindrical or conical area. The estimation of an approximate location for radionuclide 210 based solely on the detected primary photon 220 is similar to SPECT imaging. In particular, without further information (e.g. depth information) it is impractical, if not impossible, to further localize the position of the photon emission event.

[0059] Figure 3 is an illustrative schematic example of dual photon imaging in which a pair of photons is emitted from an interaction (e.g. annihilation) of a positron and an electron. In this example, as radionuclide 211 undergoes radioactive decay, a positron is emitted from radionuclide 211. This positron travels until it loses enough of its kinetic energy to interact with (i.e. annihilate) an electron; the positron may travel a distance of up to a few millimeters from its point of emission. This positron-electron annihilation event results in a pair of secondary photons 230a and 230b travelling in opposite directions (e.g. 180 degrees apart), each having an energy of γ_2

(referred to herein as a secondary energy). The energies of photons 230a and 230b are expected to be approximately 511 keV; that is, photons 230a and 230b each have a secondary expected energy of, in this example, approximately 511 keV. In Figure 3, these secondary photons are subsequently detected at detectors 200_3 and 200_9, respectively. Based on the locations on photon detectors 200_3 and 200_9 at which these secondary photons 230a and 230b are detected, an approximate location of the positron-electron annihilation event (i.e. the source of the secondary photon emission) can be estimated as being somewhere along a line of flight 232. As the positron annihilation event can be expected to occur relatively close to the location of the positron emission, the estimated location of the positron-electron annihilation event can be used as a proxy for an approximate location of the radionuclide 211 at the time of its radioactive decay. (In practice, the average distance a positron travels from its point of emission before it is annihilated can be estimated based on the expected decay energies of radionuclide/isotope 211).

[0060] Also, based on the relative time of detection for photons 230a and 230b, one can estimate at what point along line of flight 232 the annihilation event occurred. For instance, if photon 230a is detected slightly before photon 230b is detected, this implies that photon 230a travelled a shorter distance than photon 230b, and therefore the annihilation event occurred closer to detector 200_9 than to detector 200_3. For example, if $d_{3\text{-}9}$ is the distance between the two detectors 200_3 and 200_9 in Figure 3, and if we take t_3 as the time at which the photon 230a is registered at detector 200_3 and t_9 as the time at which the photon 230b is registered at detector 200_9, then we can solve for the distance between the detector 200_3 and the point at which the photons originated as follows: Let x be the distance between the detector 200_3 and the point at which the photons originated and let t_{origin} be the time of the annihilation event (i.e. the time at which the photons originate). It follows that photon 230a travels a distance x in the time $t_3 - t_{origin}$, and that photon 230b travels a distance $d_{3\text{-}9} - x$ in the time $t_9 - t_{origin}$ to reach detector 200_9.

[0061] Thus:

$$x - c \times (t_3 - t_{origin}) \qquad (3)$$

and

$$d_{3-9} - x = c \times (t_9 - t_{origin}) \qquad (4)$$

[0062] where c is the speed of a photon (i.e. approximately 3 x 10^8 m/s, or 0.3 m/ns).

[0063] Rearranging equations (3) and (4) yields:

$$x = \frac{d_{3-9} - c(t_9 - t_3)}{2} \qquad (5)$$

[0064] As d_{3-9} is the fixed distance between the detectors (i.e. a known quantity), the distance between the detector 200_3 and the point at which the photons originated (i.e. the point of emission of the photons along the line of flight 232) can be determined based on the time difference of the detection of the two photons 230a and 230b at the respective detectors 200_3 and 200_9.

[0065] In practice, based on the spatial resolution of photon detectors 200 and the temporal resolution of the data collection system, the approximate location of the positron-electron annihilation event may be estimated in three dimensions as region 234_i which may be a substantially spherical area. That is, the estimation of a location for radionuclide 211 is based on detected secondary photons 230a and 230b.

[0066] As noted above, applicants propose to employ a single radioisotope that emits positrons accompanied by photon emissions of the daughter product. As the lifetime of a photon emitting excited nuclear state is typically on the order of a sub-nanosecond time scale, the positron emission and photon emission occur at effectively the same place (since an excited 'daughter' nucleus barely moves before the photon is emitted). The positron itself may move up to about a few millimeters before it annihilates with an electron, resulting in the emission of two 511 keV photons. Accordingly, an approximation of the location of a radionuclide can be made by presuming a common emission time and a common point of origin for a primary photon and at least one secondary photon emitted from the annihilation of the positron. As discussed above, the detector location and timing information for the secondary photons can be used to approximate a locus for the positron annihilation region, and the detector location and timing information for the primary photon can be used to approximate a cylindrical or conical region for the location of the radionuclide at the time of its radioactive decay (i.e. at the time of the emission of the

primary photon). As will be discussed further below, if the location of the positron annihilation and the location of the emission of the primary photon are temporally and spatially correlated, the intersection of these two regions may localize the decay point of the radionuclide to a much narrower region. Such an approximation can be expected to be a significant improvement in comparison to estimates based solely on detection of a primary photon (e.g. SPECT imaging), or solely on detection of at least one secondary photon (e.g. PET imaging).

[0067] This can be seen, for example, in Figure 4, in which a number of photon detectors 200 are directed towards a target region 205 that contains a radionuclide 212. As this radionuclide 212 undergoes radioactive decay, a primary photon 220 having an energy γ_1 (referred to herein as a primary energy) is emitted and subsequently detected at detector 200_1. As explained above with reference to Figure 2, based on the location of photon detector 200_1 at which this primary photon 220 is detected, an approximate location of the radionuclide 212 at the time of its radioactive decay (i.e. the source of the primary photon emission) can be estimated as being within the three dimensional region 224.

[0068] At nearly the same instant – but slightly before – the primary photon is emitted (on the order of a few picoseconds or less) a positron is also emitted from radionuclide 212. This positron travels until it loses enough of its kinetic energy to interact with (i.e. annihilate) an electron; the positron may travel a distance of up to a few millimeters from its point of emission. This positron-electron annihilation event results in a pair of secondary photons 230a and 230b travelling in opposite directions (e.g. 180 degrees apart), each having an energy of γ_2 (expected to be approximately 511 keV). These secondary photons are subsequently detected at detectors 200_3 and 200_9, respectively. As explained above with reference to Figure 3, based on the locations on photon detectors 200_3 and 200_9, and optionally based on the relative time of detection for photons 230a and 230b (as discussed above), an approximate location of the positron-electron annihilation event may be estimated in three dimensions as region 234, which may be a substantially spherical area. Also, as the time at which the primary photon 220 is detected at detector 200_1 (e.g. t_1) will be recorded, this information may further assist in localizing the decay and annihilation points.

[0069] By using a radionuclide that emits a photon and a positron at nearly the same instant, the time of emission of the primary photon 220 and the time of emission of the secondary photons 230a and 230b is highly correlated. Similarly, the location of emission of the primary photon 220 and the location of emission of the secondary photons 230a and 230b (i.e. the photons produced by positron annihilation) is also highly correlated. If the primary photon and the secondary photons are considered to originate from the same location (i.e. have a common point of origin), the approximate location of this point of origin can be determined based on the intersection 244 of areas 224 and 234. That is, an approximate location for radionuclide 212 at the time of its radioactive decay can be determined based on both the primary photon 220 and the secondary photons 230a and 230b.

[0070] While none of Figures 2 to 5 are to scale, it can be expected that the approximate location for radionuclide 212 at the time of its radioactive decay determined based on a correlation (e.g. a presumed common point of origin) of photons 220, 230a, and 230b (e.g. area 244) will be a significantly improved estimate over approximate locations based on single photon 220 (e.g. area 224) or dual photons 230a, 230b (e.g. area 234).

[0071] Of course, Figures 2 to 5 are only illustrative schematic examples, and actual detector systems may vary. For example, there may be more or fewer photon detectors 200 in each detector ring, and there may be more than one detector ring located about a common axis, forming a cylinder of detector elements.

[0072] Persons skilled in the art will also recognize that a number of radionuclides may be introduced into a target region of a detector array, and that a volumetric image may be reconstructed based on an analysis of approximate locations determined for a number of decay events detected within the target region.

[0073] In some embodiments, a detector system similar to what is currently being used in PET imaging may be used. For example, a cluster of scintillation detectors or solid state detectors or combinations thereof 200_1, 200_2,.....200_N may be used to generate fast time signals and linear energy signals. A schematic block diagram of such a detector system 300 is shown in Figure 6. The blocks 200_1, 200_2,.....200_N are photon detectors, each sending analog signals carrying energy information to amplifiers 310_1, 310_2,.....310_N, which may be linear amplifiers.

Amplifiers 310 shape and amplify the signals received from the detectors 200, and preferably maintain a linear relationship between the output amplitude and the detector output. . The output of amplifier 310 - generally a slow pulse of a few microseconds width (<2-5 microseconds)- with appropriate time delay conditions is fed as input to an Analog Digital Converter (ADC), as discussed further below.

[0074] The photon detectors 200_1, 200_2,.....200_N also each send fast logic signals with time information to discriminators 320_1, 320_2,.....320_N. These discriminators generate a fast output (<10 nano seconds) logic signal upon receipt of input from the detector. In some embodiments, a threshold level can be programmed or otherwise set. The threshold level is a voltage above which the discriminator is operative to generate an output, and in some embodiments may be as low as a few tens of milli Volts. Discriminators 320 generate two or more outputs, at least one of which will be analyzed by the majority logic unit (MLU) 330 to determine the number of detectors outputting signals.

[0075] The MLU 330 accepts the logic signals from the discriminators 320. The timing resolution of MLU 330 is generally determined by the pulse widths of the input signals received from the discriminators, which may be approximately 10 nanoseconds. In some systems MLU 330 may comprise a Field Programmable Gate Array (FPGA) for versatility of logical analyses in a simple setting.

[0076] The logic condition of MLU 330 may be configured such that it generates output for a photon detection event that corresponds to a preset logic requirement. For example, MLU 330 may generate an output signal if 1, 2, or 3 photons are simultaneously (or near-simultaneously) detected – that is, a detection event may occur when 1, 2, or 3 logic inputs are received from discriminators 320. Alternatively, MLU 330 may be configured to generate an output signal if a minimum number of time adjusted input signals from the discriminators are received (e.g. if at least 1, 2, or 3 input signals are received). The conditions for satisfying a detection event may also include a minimum energy level output by a detector 200, or other conditions.

[0077] The MLU signal is fed to a Gate Generator (GG) 340 which may perform pulse shaping (polarity, height, shape and width) on the signal received from

the MLU 330 to serve as trigger pulses to the Time to Digital Converter (TDC) 360. In some embodiments, GG 340 may be integrated into MLU 330.

[0078] TDC 360 registers time information for the photon detection events. TDC 360 is triggered by the signals received from GG 340, and also receives time-adjusted logical signals from the discriminators 320_1, 320_2 ... 320_N as input signals. The timing information registered by TDC 360 is relative to the GG trigger pulse and arrival times of all individual photon detection signals and an address identifying the detector at which the photon detection signal was detected (e.g. at which detector 200_1, 200_2, ... 200_N the signal was registered) are recorded.

[0079] The output signal from GG 340 is also fed as a trigger to the Analog Digital Converter (ADC) 350, which also receives time-adjusted linear signals from the amplifiers 310_1, 310_2,.....310_N. Receipt of a trigger pulse from GG 340 sets ADC 350 in an "active mode" for a predetermined time interval, during which ADC 350 receive pulses from amplifiers 310 as inputs. In some embodiments, the conversion times of the ADC and TDC modules may be of the order of a few microseconds. The predetermined time interval for recording a detection event may last from about 100 nanoseconds to about a few microseconds. While ADC 350 is in active mode, it converts the analog pulses from the amplifiers 310 containing energy information into digital pulse signals that may be stored along with the corresponding detector addresses and arrival times registered by the TDC 360. This information – i.e. the arrival time(s), detector location(s), and energy information for each detection event that satisfies the logic conditions of MLU 330/GG 340 – may be fed to a computer 370 for further data processing.

[0080] Of course, Figure 6 is only an illustrative schematic example, and actual detector systems and electronic arrangements may vary. For example, FPGAs or other hardware or software logic elements may be used in combination to detect and record photon emissions from target region 205.

[0081] In some embodiments, detector system 300 may include a processor or processors (not shown) and computer readable storage media (not shown) with instructions stored thereon to instruct the processor(s) to register the energy and time of arrival information of photons at each detector, with data being recorded in list-mode. For example, this information may be sent to a list-mode data buffer. In

the list-mode, the following information may be recorded for each detection event: i) the number of photon detectors outputting an energy signal indicative of a photon detection; ii) the identity (e.g. address) of each of these detectors; iii) energy information for each of these detectors as recorded by the ADC 350 channels; and iv) time information for each of these detectors as recorded by the TDC 360 channels. In some embodiments, the hardware logic of a typical PET detector system may be modified to allow for list-mode or other forms of data collection.

[0082] In list-mode data acquisition, each detection event may be recorded in, for example, a data array. This data array may include the following information: Number (e.g. ID) of each detector registering a photon, the time of arrival of that photon at that detector, the energy deposited by the photon at the detector. A person skilled in the art will recognize that more or less information may be recorded.

[0083] By collecting data in such a list-mode, the data may be analyzed to distinguish detection events based on, for example, the relative time of arrival of two or more photons, the energies of detected photons, or both. In this way, if only a single photon is detected during a detection event (i.e. during the predetermined time interval discussed above), it may be possible to determine if this detected photon is a primary photon (e.g. analogous to a SPECT photon) or one of a pair of secondary photons (e.g. one of a pair of PET photons, the other having not been successfully detected) based on the energy information recorded for that detection event. Similarly, where two photons are detected during a detection event, it may be possible to determine if this represents the detection of a pair of secondary photons (e.g. analogous to PET photons) or if one primary photon and one secondary photon have been detected (e.g. where one of the secondary photons was not detected – this may occur, for example, if one of the secondary photons is deflected before reaching the detectors) from the energy information. Similarly, where three photons are detected during a recorded detection event, the relative energies of the detected photons can be used to confirm that a primary photon and a pair of secondary photons – presumed to originate from the same decay event – have been detected.

[0084] In some embodiments, where a primary photon and at least one secondary photon are detected within the predetermined time interval (i.e. their emission is temporally correlated), as discussed above they may be presumed to

share a common point of origin (i.e. their emission locations are spatially correlated) and an approximate location for the radionuclide at the time of its radioactive decay can be determined based on this presumption. With a data set comprising approximate locations for temporally and spatially correlated decay events, a volumetric reconstruction (e.g. tomographic reconstruction) of such a data set may reduce, or correct for, one or more imaging 'artifacts' of concern to radiologists that may be present in images reconstructed in typical PET or SPECT systems.

[0085] In some embodiments, the list-mode data may be parsed to separate the detection information for photons having the primary energy from the detection information for photons having the secondary energy (e.g. 511 keV). In this way, either a SPECT image or a PET image (or both) may be separately reconstructed from the data set collected during a single scanning procedure.

[0086] For example, the list-mode data set may be analyzed to identify detection events during which three photons were detected, and these three-photon detection events may be further analyzed to identify detection events during which one primary photon and two secondary photons were detected. As discussed above, a volumetric reconstruction (e.g. tomographic reconstruction) of such a data set can be expected to provide a more accurate representation – based in the improved approximate locations of the radionuclides – than images reconstructed in typical PET or SPECT systems. Subsequently, one can take the same data set of three-photon (one primary, two secondary) detection events and remove or otherwise ignore the information regarding the primary photons and reconstruct a volumetric image based only on the detected secondary photons (as in typical PET imaging) and compare this two-photon PET image with the three-photon image. Such a comparison may be useful in identifying imaging artifacts or other undesirable imaging sensitivities that may not be identifiable by traditional imaging systems. Alternatively, the data set of three-photon (one primary, two secondary) detection events can be analyzed to remove or otherwise ignore the information regarding the secondary photons and reconstruct a volumetric image based only on the detected primary photons (as in typical SPECT imaging) and compare this one-photon PET image with the three-photon image. Again, such a comparison may be useful in

identifying imaging artifacts or other undesirable imaging sensitivities that may not be identifiable by traditional imaging systems.

[0087] In some embodiments, the image analysis performed will be similar to that of typical SPECT and PET software. In order to accommodate PET, SPECT and PET/SPECT imaging from the same data set, various exemplary types of imaging are outlined as follows.

[0088] In a first type of imaging, [Type A], one photon is detected during the predetermined time interval. If the detected photon has a secondary energy (i.e. the photon is a product of a positron-electron annihilation) an approximate location of the positron at the time of its annihilation may be determined assuming that the other secondary photon went undetected. While the approximate location based on a single photon may be determined as discussed above with reference to Figure 2, it may be possible to take into consideration the different expected attenuation for a 511 keV photon (compared to the expected attenuation for a lower energy photon). Reconstructing a volumetric image based on detected photons having a secondary energy (e.g. 511 keV) may be regarded as Type A (high energy) SPECT imaging.

[0089] If the one photon detected during the predetermined time interval has a primary energy, the system may employ a SPECT imaging mode – i.e. determine approximate locations for decay events based on one detected photon per decay event – and the resulting image will be similar to a conventional SPECT image. Reconstructing a volumetric image based on detected photons having a primary energy may be regarded as Type A (low energy) SPECT imaging.

[0090] Comparing and/or combining Type A (high energy) and Type A (low energy) images may therefore constitute a form of dual energy SPECT imaging.

[0091] In a second type of imaging, [Type B], two photons are detected during the predetermined time interval. If both detected photons have the expected energy of a secondary photon (e.g. 511 keV), the system will employ a PET imaging mode – i.e. determine approximate locations for decay events based on two detected photons per decay event – and the resulting image will be similar to a conventional PET image. For example, as shown in Figure 5, if secondary photons 230a and 230b are detected at detectors 200_3 and 200_7, respectively, but primary photon 220 is not

detected, an approximate location for the radionuclide may be estimated in three dimensions as region 234a.

[0092] Alternatively, if one detected photon has a secondary energy and the other detected photon has a primary energy, by presuming a correlation between the emission of the primary photon and the positron annihilation (e.g. by presuming a common point of origin) a location of the radionuclide at least as accurate as in Type A may be determined. For example, as shown in Figure 5, if primary photon 220 is detected at detector 200_1 and secondary photon 230a is detected at detector 200_3, but secondary photon 230b is not detected, an approximate location for the radionuclide at the time of its decay may be estimated in three dimensions as region 244a (i.e. the intersection of areas 224a and 224b)..

[0093] In a third type of imaging, [Type C], three photons are detected during the predetermined time interval, and information for each of the three photons is used to determine approximate locations of the decay events (as discussed above with reference to Figure 4). For example, as shown in Figure 5, if all three photons 220, 230a and 230b are detected at detectors 200_1, 200_3, and 200_7, respectively, an approximate location for the radionuclide at the time of its decay may be estimated in three dimensions as region 244b (i.e. the intersection of areas 224a and 234b, region 234b being estimated based on the presumed correlation between the emission location of the primary photon and the positron annihilation event, which implies that the region 234b and 224a should intersect).

[0094] In a fourth type of imaging, [Type D], three photons are detected during the predetermined time interval, as in Type C. However, unlike in Type C, information from only two of the three detected photons is used to determine approximate locations of the decay events. That is, the detection information recorded for a primary photon may be suppressed or ignored, and an approximate location of the decay event may be based on the two secondary photons, as discussed above. Alternatively, detection information recorded for one of the two detected secondary photons may be suppressed or ignored, and an approximate location of the decay event may be based on the primary photon and the other one of the two detected secondary photons (as in Type B). That is, in Type D the detection information recorded for a primary photon or a secondary photon is not

utilized in the image reconstruction. The differences in the images obtained in this manner and the images reconstructed using the Type C imaging may assist in the identification and/or classification of imaging artifacts. Alternatively (or additionally), images produced using Type D imaging may be compared with images produced using Type B imaging to verify the robustness of the imaging algorithms - as the Type B and Type D images should be similar (if not identical) as they are based on the same information, consistency between the Type B and Type D images may increase the confidence in Type B imaging where the additional Type D data is unavailable.

[0095] In a fifth type of imaging, [Type E], three photons are detected during the predetermined time interval, as in Types C and D. However, information from only one of the three detected photons is used to determine approximate locations of the decay events. For example, the detection information recorded for the secondary photons may be suppressed or ignored, and an approximate location of the decay event may be based on the primary photon, as in SPECT imaging. Alternatively, detection information recorded for the primary photon and one of the two detected secondary photons may be suppressed or ignored, and an approximate location of the decay event may be based on the other secondary photon (as in Type A). That is, in Type E the detection information recorded for two of the three detected photons is not utilized in the image reconstruction. The differences in the images obtained in this manner and the images reconstructed using the Type C imaging may assist in the identification and/or classification of imaging artifacts. Alternatively (or additionally), images produced using Type E imaging may be compared with images produced using Type A imaging to verify the robustness of the imaging algorithms - as the Type A and Type E images should be similar (if not identical) as they are based on the same information, consistency between the Type A and Type E images may increase the confidence in Type A imaging where the additional Type E data is unavailable.

[0096] Use of one or more of the above imaging types may also contribute to improving detector assemblies and/or imaging algorithms. For example, images generated using data collected at a first section of a detector assembly (e.g. the upper half of a cylindrical detector array) may be compared to images generated

using data collected from a second section (e.g. the lower half of the array). If Type A (high energy) images generated using data collected at the first and second sections appear identical (or nearly identical), but appear different from Type A (low energy) images generated using data collected at the first and second sections, we may attribute the differences to energy-dependent attenuation artifacts. However, if the Type A (high energy) image generated using data collected at the first section appears different from the Type A (high energy) image generated using data collected at the second section, detector geometry may be considered a contributing factor.

[0097] Through the use of one or more of the above imaging types, artifacts of scattering present in PET or SPECT imaging or both may be analyzed more thoroughly than in known systems. That is, the proposed imaging types may allow for cross-checking image information in multiple ways, which may reduce ambiguity in interpreting the data. For example, this may involve recovering PET-only and SPECT-only imaging in order to assess the consistency of the data and to assess energy dependent artifacts of scattering and absorption in different physiological zones of a patient. For example, the primary (SPECT) photons are subject to absorption in bone, however they typically pass through soft tissue with scattering – not absorption - effects. Contrastingly, the secondary (PET) photons of higher energy typically are not significantly attenuated by passing through soft tissue. Secondary photons are also likely to pass through bone also without significant absorption, but they may be subject to scattering.

[0098] In some embodiments, a medical practitioner may be presented with images based on one or more of the above imaging types on different monitors. The practitioner may then examine these images and critically evaluate the influence of imaging artifacts and arrive at more reliable diagnostic information. This may provide a better check of the computer imaging algorithms for their correctness and accuracy, and may provide an improved basis for the evaluation of influences of different physiological components on the passage of gamma radiation through tissue and bone. This information may reduce diagnostic errors relating to either false positives (scattering), false negatives (absorption), or other errors induced by imaging artifacts.

ISOTOPE SELECTION

[0099] As noted above, in order to collect temporally and spatially correlated gamma emission data, a single radioisotope that emits positrons accompanied by photon emissions of the daughter product is used. In order to be useful in medical imaging, a radioactive isotope should meet several criteria.

[00100] First, the half-life of the radionuclides should be neither too short nor too long (optimal ones are about a few hours). If the half-life is too short, there is not enough time for the radionuclides to be processed and injected into a patient, and if the half-life is too long, the residual radio-activities after imaging maybe too high and be of adverse health concerns.

[00101] Second, the production rate (which is a product of the isotope abundance and production cross section) should be high enough to ensure a sufficient amount of the isotope can be manufactured for each scan.

[00102] Third, the primary photon should be expected to have an energy sufficiently different from the secondary photons for contrast reasons. For medical imaging, it is preferable that the primary photon has an expected energy lower than the expected energy of the secondary photons (e.g. less than about 511 KeV), as a photon with too high of an energy will simply pass through the bone and soft tissue without any contrast.

[00103] Fourth, the primary photon should have a comparable intensity to the secondary photons to accomplish an effective PET/SPECT photon imaging.

[00104] Fifth, for medical imaging applications, the isotope should be compatible with the human body. For example, it should be able to be incorporated into a larger radioactive tracer molecule (e.g. a metabolic substrate, receptor ligand, antibody, organic molecule, amino acid, or polypeptide), administrable directly (e.g. as a soluble ionic salt), or otherwise be incorporated into a radiopharmaceutical.

[00105] Based on the foregoing criteria, ^{123}Xe, ^{73}Se, ^{75}Br, ^{174}Ta, ^{99}Rh, and ^{184}Ir have been identified as potentially suitable isotopes for medical imaging in accordance with aspects as described herein.

[00106] In order to identify potentially useful isotopes an initial list of 116 photon and positron emitters having half-lives from about 1 to about 10 hours was examined

from the database available from the National Nuclear Data Center (NNDC) at the Brookhaven National Laboratory. Out of these 116 isotopes, 17 isotopes were chosen and ranked based on the half-life and intensity criteria discussed above (see Table 1). Some isotopes were eliminated because either the 511 keV gamma lines or the primary photons did not have large enough intensities to be useful for PET/SPECT imaging. Isotopes must have at least one gamma ray with sufficient intensity in addition to the annihilation 511 keV photons.

Table 1

Isotope	Half-life (t½)	Daughter Nucleus	Eγ (keV)	Iγ (%)
^{81}Rb*****	4.572 h	81Kr	12.598	17
			12.651	33
			190.46	64.9
			446.15	23.5
			511	54.4
^{123}Xe****	2.08 h	123I	28.317	20.8
			28.612	38.4
			148.9	48.9
			178.1	14.9
			511	45.1
^{43}Sc***	3.891 h	43Ca	372.9	22.5
			511	176.2
^{66}Ge***	2.26 h	66Ga	9.225	14.7
			9.252	28.9
			43.89	29.1
			108.85	10.6
			381.85	28.3
			511	47
^{73}Se***	7.15 h	73As	10.54	16.1
			67.07	70
			361.2	97
			511	130.8
^{75}Br***	96.7 m	75Se -> 75As	286.50	90
			511	146
^{90}Mo***	5.67 h	90Nb	16.521	24.4
			16.615	46.6
			122.37	64
			257.34	78
			511	50
^{174}Ta***	1.14 h	174Hf	7.9	36.3
			54.07	43

			54.611	24.8
			91	15.9
			206.5	60
			511	47
^{61}Cu**	3.333 h	61Ni	282.956	12.2
			511	123
^{77}Kr**	74.4 m	77Br	11.924	10.7
			129.64	81
			146.59	37.3
			511	163
^{82m}Rb**	6.472 h	82Kr	12.598	13.4
			12.651	25.9
			511	42
			554.35	62.4
			619.11	37.98
			698.37	26.3
			776.52	84.39
			827.83	21
			1044.08	32.07
			1317.43	23.7
			1474.88	15.5
^{85}Y**	4.86 h	85Sr	14.165	14.6
			231.7	22.8
			511	116
^{95}Ru**	1.643 h	95Tc	18.251	17.2
			18.367	32.7
			336.4	70.2
			511	28
			626.83	17.8
			1096.8	21
^{99}Rh**	4.7 h	99Ru	19.15	19.7
			19.279	37.4
			340.8	70
			511	14.8
			617.8	12
			1261.2	11.1
^{121}I**	2.12 h	121Te	27.202	20.9
			27.472	38.6
			212.2	84.3
			511	21.2
^{173}Ta**	3.14 h	173Hf	7.9	47
			54.07	60
			54.611	34.4
			63.243	12.8

			172.2	17.5
			511	13.7
$^{184}Ir^{**}$	3.09 h	184Os	8.91	40.9
			61.486	26.9
			63	45.8
			71.414	10.4
			119.79	30.8
			263.98	64.4
			390.36	26.1
			511	24.7
			961.26	10.2

[00107] Next, possible production methods were examined for these 17 isotopes. Cross section data for the proton and photon induced reactions (p,xn) and (γ,xn) processes were obtained from the NNDC database. Where experimental data was not available, cross sections were determined by taking advantage of the systematic properties of giant resonances, which have been studied by the nuclear physics community for more than half a century. That is, maximum cross section is present in the giant resonance region where excitation energy is given by $E_x=77 \times A^{-1/3}$ MeV, where A is the mass number. Therefore, the cross section for neighboring nuclides that share a similar mass number ($A_{reference}/A_{isotope} \approx 1$) can be used to estimate cross section for an isotope of interest:

$$ {}^{A}_{Z}a + p \rightarrow {}^{A+1}_{Z+1}b^{*} \rightarrow {}_{Z+1}{}^{A}b + n $$

[00108] The energetics of reaction influence the cross sections in a drastic way. To ensure that the reaction energetics of the isotope production are similar to that of the reference isotope, we compared the energy release (a Q-value) for the capture process (p,γ) on the reference target. As long as $Q^{isotope}_{(p,\gamma)} \approx Q^{reference}_{(p,\gamma)}$, it can be assumed that $\sigma_{reference} \approx \sigma_{isotope}$.

[00109] Table 2 shows cross sections for (p,xn) reactions:

Table 2

	Reaction	Q-value for (p,γ) reaction (MeV)	Cross section, σ (barns)	Energy of protons (MeV)
Reaction of Interest	$^{174}Hf(p,n)^{174}Ta$	3.851	No data	No data

Reactions of Neighbouring Nuclides	$^{178}Hf(p,n)^{178}Ta$	5.211	0.06	9
	$^{180}Hf(p,n)^{180}Ta$	5.942	0.1	9
	$^{181}Ta(p,n)^{180}W$	7.095	0.1	10
	$^{169}Tm(p,n)^{180}Yb$	6.778	0.28	11
	$^{168}Er(p,n)^{180}Tm$	5.572	0.25	11
	$^{165}Ho(p,n)^{180}Er$	7.316	0.15	11
Reaction of Interest	$^{176}Hf(p,3n)^{174}Ta$	3.851	No data	No data
Neighbouring Nuclides	$^{181}Ta(p,3n)^{179}W$	7.095	0.8	25
	$^{169}Tm(p,3n)^{167}Yb$	6.778	0.8	25
	$^{153}Eu(p,3n)^{151}Gd$	7.629	0.9	25
Reaction of Interest	$^{177}Hf(p,4n)^{174}Ta$	3.851	No data	No data
Neighbouring Nuclides	$^{181}Ta(p,4n)^{178}W$	7.095	0.7	35
	$^{192}Os(p,4n)^{189}Ir$	5.942	0.9	35
	$^{169}Tm(p,4n)^{166}Yb$	6.778	0.6	38
Reaction of interest	$^{178}Hf(p,5n)^{174}Ta$	5.211	No data	No data
Neighbouring Nuclides	$^{181}Ta(p,5n)^{177}W$	7.095	0.06	100
	$^{192}Os(p,5n)^{188}Ir$	5.942	0.9	43
Reaction of interest	$^{86}Kr(p,5n)^{82}Rb$	8.621	No data	No data
Neighbouring Nuclides	$^{81}Br(p,5n)^{77}Kr$	9.904	0.04	60
	$^{85}Rb(p,5n)^{81}Sr$	9.645	0.03	67
	$^{88}Sr(p,5n)^{84}Y$	7.069	0.025	69
Reaction of interest	$^{87}Sr(p,3n)^{85}Y$	6.707	No data	No data
Neighbouring Nuclides	$^{84}Kr(p,3n)^{82}Rb$	7.025	0.2	30
	$^{86}Kr(p,3n)^{84}Rb$	8.621	0.5	30
	$^{85}Rb(p,3n)^{83}Sr$	9.645	0.45	35
	$^{88}Sr(p,3n)^{86}Y$	7.069	0.3	36
	$^{89}Y(p,3n)^{87}Zr$	8.354	0.35	38
Reaction of interest	$^{100}Ru(p,2n)^{99}Rh$	5.478	No data	No data
Neighbouring Nuclides	$^{95}Mo(p,2n)^{94}Tc$	5.399	0.5	22
	$^{96}Mo(p,2n)^{95}Tc$	5.719	1	20
	$^{97}Mo(p,2n)^{96}Tc$	6.176	1.2	19
	$^{100}Mo(p,2n)^{99}Tc$	7.441	0.35	17
Reaction of interest	$^{101}Ru(p,3n)^{99}Rh$	6.114	No data	No data
Neighbouring Nuclides	$^{96}Mo(p,3n)^{94}Tc$	5.719	0.5	30
	$^{97}Mo(p,3n)^{95}Tc$	6.176	0.7	28
	$^{98}Mo(p,3n)^{96}Tc$	6.500	0.95	30
	$^{99}Tc(p,3n)^{97}Ru$	9.185	0.4	30
	$^{103}Rh(p,3n)^{101}Pd$	8.657	0.55	28
Reaction of interest	$^{102}Ru(p,4n)^{99}Rh$	6.213	No data	No data

Neighbouring Nuclides	$^{96}Mo(p,4n)^{93}Tc$	5.719	0.3	45
	$^{103}Rh(p,4n)^{101}Pd$	8.657	0.28	40
Reaction of interest	$^{104}Ru(p,6n)^{99}Rh$	7.046	No data	No data
Neighbouring Nuclide	$^{116}Cd(p,6n)^{111}In$	7.515	0.13	70
Reaction of interest	$^{123}Te(p,3n)^{121}I$	5.482	No data	No data
Neighbouring Nuclides	$^{120}Sn(p,3n)^{118}Sb$	5.779	0.002	4
	$^{124}Sn(p,3n)^{122}Sb$	7.308	0.004	4
	$^{122}Te(p,3n)^{120}I$	4.918	0.5	34
	$^{125}Te(p,3n)^{123}I$	6.177	0.9	32
	$^{126}Te(p,3n)^{124}I$	6.208	1.6	30
Reaction of interest	$^{174}Hf(p,2n)^{173}Ta$	3.851	No data	No data
Neighbouring Nuclides	$^{166}Er(p,2n)^{165}Tm$	4.906	0.9	15
	$^{167}Er(p,2n)^{166}Tm$	5.310	0.8	15
	$^{181}Ta(p,2n)^{180}W$	7.095	0.8	14
Reaction of interest	$^{176}Hf(p,4n)^{173}Ta$	4.435	No data	No data
Neighbouring Nuclides	$^{169}Tm(p,4n)^{166}Yb$	6.778	0.6	40
	$^{181}Ta(p,4n)^{178}W$	7.095	0.7	36
Reaction of interest	$^{177}Hf(p,5n)^{173}Ta$	4.907	No data	No data
Neighbouring Nuclide	$^{181}Ta(p,5n)^{177}W$	7.095	0.06	100
Reaction of interest	$^{184}Os(p,n)^{184}Ir$	3.368	No data	No data
Neighbouring Nuclides	$^{178}Hf(p,n)^{178}Ta$	5.211	0.065	9
	$^{180}Hf(p,n)^{180}Ta$	5.942	0.1	9
	$^{181}Ta(p,n)^{181}W$	7.095	0.1	10
	$^{186}W(p,n)^{186}Re$	5.995	0.15	10
Reaction of interest	$^{186}Os(p,3n)^{184}Ir$	4.005	No data	No data
Neighbouring Nuclides	$^{181}Ta(p,3n)^{179}W$	7.095	0.85	24
	$^{192}Os(p,3n)^{190}Ir$	5.942	1.2	24
Reaction of interest	$^{187}Os(p,4n)^{184}Ir$	4.399	No data	No data
Neighbouring Nuclides	$^{181}Ta(p,4n)^{178}W$	7.095	0.7	35
	$^{192}Os(p,4n)^{189}Ir$	5.942	0.9	35
Reaction of interest	$^{188}Os(p,5n)^{184}Ir$	4.606	No data	No data
Neighbouring Nuclides	$^{181}Ta(p,5n)^{177}W$	7.095	0.06	100
	$^{192}Os(p,5n)^{188}Ir$	5.942	0.9	43
Reaction of interest	$^{189}Os(p,6n)^{184}Ir$	5.055	No data	No data
Neighbouring Nuclides	$^{192}Os(p,6n)^{187}Ir$	5.942	0.55	55
	$^{197}Au(p,6n)^{192}Hg$	7.102	0.005	500

Reaction of interest	$^{190}Os(p,7n)^{184}Ir$	5.289	No data	No data
Neighbouring Nuclides	$^{192}Os(p,7n)^{186}Ir$	5.942	0.3	67
	$^{206}Pb(p,7n)^{200}Bi$	3.558	0.18	64

[00110] Similarly, cross sections determined for (γ,xn) reactions are shown in Table 3:

Table 3

	Reaction	Q-value for reaction (MeV)	Cross section, σ (barns)	Energy of gammas (MeV)
Reaction of Interest	$^{85}Rb(\gamma,3n)^{82}Rb$	-30.193	No data	No data
Neighbouring Nuclide	$^{94}Zr(\gamma,3n)^{91}Zr$	-23.590	0.01	29
Reaction of Interest	$^{89}Y(\gamma,4n)^{85}Y$	-42.145	No data	No data
Neighbouring Nuclide	$^{93}Nb(\gamma,4n)^{89}Nb$	-38.843	0.0002	150
Reaction of Interest	$^{98}Ru(\gamma,n)^{95}Ru$	-10.694	No data	No data
Neighbouring Nuclides	$^{94}Mo(\gamma,n)^{93}Mo$	-9.678	0.18	16
	$^{96}Mo(\gamma,n)^{95}Mo$	-9.154	0.19	16
	$^{98}Mo(\gamma,n)^{97}Mo$	-8.643	0.18	16
Reaction of Interest	$^{98}Ru(\gamma,3n)^{95}Ru$	-28.989	No data	No data
Neighbouring Nuclides	$^{96}Mo(\gamma,3n)^{93}Mo$	-26.201	0.01	29
	$^{98}Mo(\gamma,3n)^{95}Mo$	-24.618	0.013	28
	$^{100}Mo(\gamma,3n)^{97}Mo$	-22.858	0.023	28
Reaction of Interest	$^{99}Ru(\gamma,4n)^{95}Ru$	-36.452	No data	No data
Neighbouring Nuclide	$^{93}Nb(\gamma,4n)^{89}Nb$	-38.843	0.0002	150

[00111] A production quality factor ($Q_{production}$) was then determined for each of the 17 isotopes by multiplying the maximum cross section (in barns) by the abundance of the isotope (expressed as a percentage). The results are shown below in Table 4.

Table 4

Isotope of Interest	Production Method	Maximum Cross Section, σ	Corresponding Energy of Protons or	Abundance of Isotope, ϑ (%)	Quality Factor σ x ϑ

		(barns)	Gammas(MeV)		(2 sig figs)
^{81}Rb	^{82}Kr(p,2n)^{81}Rb	0.55	20	11.58	6.4
^{123}Xe	^{127}I(p,5n)^{123}Xe	0.4	55	100	40
^{43}Sc	^{44}Ca(p,2n)^{43}Sc	0.15	22	2.09	0.31
^{66}Ge	^{69}Ga(p,4n)^{66}Ge	0.008	50	60.108	0.48
^{73}Se	^{74}Se(γ,n)^{73}Se	0.09	16	0.89	0.080
	^{75}As(p,3n)^{73}Se	0.35	35	100	35
^{75}Br	^{76}Se(p,2n)^{75}Br	0.4	25	9.37	3.7
	^{77}Se(p,3n)^{75}Br	0.3	35	7.63	2.3
	^{74}Se(p,γ)^{75}Br	0.003	3.5	0.89	0.0027
^{90}Mo	^{93}Nb(p,4n)^{90}Mo	0.045	51	100	4.5
	^{92}Mo(γ,2n)^{90}Mo	0.005	20	14.84	0.074
^{174}Ta	^{174}Hf(p,n)^{174}Ta	0.2*	5**	0.16	0.032
	^{176}Hf(p,3n)^{174}Ta	1*	20**	5.26	5.3
	^{177}Hf(p,4n)^{174}Ta	1*	26**	18.60	19
	^{178}Hf(p,5n)^{174}Ta	1*	34**	27.28	27
^{61}Cu	^{61}Ni(p,n)^{61}Cu	0.5	10	1.140	0.57
	^{62}Ni(p,2n)^{61}Cu	0.4	25	3.634	1.5
	^{63}Cu(γ,2n)^{61}Cu	0.015	23	69.17	1.0
^{77}Kr	^{79}Br(p,3n)^{77}Kr	0.25	30	50.69	13
	^{81}Br(p,5n)^{77}Kr	0.04	60	49.31	2.0
^{82m}Rb	^{82}Kr(p,n)^{82}Rb	0.4	12	11.58	4.6
	^{83}Kr(p,2n)^{82}Rb	0.45	23	11.49	5.2
	^{84}Kr(p,3n)^{82}Rb	0.25	30	57.00	14
	^{86}Kr(p,5n)^{82}Rb	0.04*	41**	17.30	0.69
	^{85}Rb(γ,3n)^{82}Rb	0.01*	30**	72.17	0.72
^{85}Y	^{86}Sr(p,2n)^{85}Y	0.5	25	9.86	5.0
	^{87}Sr(p,3n)^{85}Y	0.5*	24**	7.00	3.5
	^{88}Sr(p,4n)^{85}Y	0.1	55	82.58	8.3
	^{89}Y(γ,4n)^{85}Y	0.0002*	42**	100	0.02
^{95}Ru	^{96}Ru(γ,n)^{95}Ru	0.2*	11**	5.54	1.1
	^{98}Ru(γ,3n)^{95}Ru	0.01*	29**	1.87	0.019
	^{99}Ru(γ,4n)^{95}Ru	0.0002*	36**	12.76	0.0026
^{99}Rh	^{99}Ru(p,n)^{99}Rh	0.5	9	12.76	6.4
	^{100}Ru(p,2n)^{99}Rh	1*	13**	12.60	13
	^{101}Ru(p,3n)^{99}Rh	0.7*	19**	17.06	12
	^{102}Ru(p,4n)^{99}Rh	0.3*	29**	31.55	9.5
	^{104}Ru(p,6n)^{99}Rh	0.1*	44**	18.62	1.9
^{121}I	^{122}Te(p,2n)^{121}I	1	25	2.55	2.6
	^{123}Te(p,3n)^{121}I	1*	20**	0.89	0.89
^{173}Ta	^{174}Hf(p,2n)^{173}Ta	1*	12**	0.16	0.16
	^{176}Hf(p,4n)^{173}Ta	0.6*	27**	5.26	3.2
	^{177}Hf(p,5n)^{173}Ta	0.05*	34**	18.60	0.93
^{184}Ir	^{184}Os(p,n)^{184}Ir	0.1*	5**	0.02	0.002
	^{186}Os(p,3n)^{184}Ir	1*	20**	1.59	1.6
	^{187}Os(p,4n)^{184}Ir	1*	27**	1.6	1.6
	^{188}Os(p,5n)^{184}Ir	1*	35**	13.29	13

	$^{189}Os(p,6n)^{184}Ir$	0.5*	41**	16.21	8.1
	$^{190}Os(p,7n)^{184}Ir$	0.3*	49**	26.36	7.9

*Maximum cross section estimated from systematics
**Threshold energy for reaction; energy of protons or gammas should be greater than threshold energy

[00112] Next, applicants quantitatively analyzed potential PET/SPECT isotopes based on the intensities of the emitted gamma rays. First, intensity ratios were determined according to the following formula:

$$Intensity\ Ratio = \frac{I(E_\gamma)}{I(511keV)} \quad (6)$$

[00113] Determined intensity ratios are shown in Table 5.

Table 5

Isotope	Eγ (kev)	Iγ (Eγ) (%)	Iγ (511 keV) (%)	Intensity ratio
^{81}Rb	190.46	64.9	54.4	1.19
	446.15	23.5	54.4	0.43
^{123}Xe	148.9	48.9	45.1	1.08
	178.1	14.9	45.1	0.33
^{43}Sc	372.9	22.5	176.2	0.13
^{66}Ge	43.89	29.1	47	0.62
	108.85	10.6	47	0.23
	381.85	28.3	47	0.60
^{73}Se	67.07	70	130.8	0.54
	361.2	97	130.8	0.74
^{75}Br	286.5	90	146	0.62
^{90}Mo	122.37	64	50	1.28
	257.34	78	50	1.56
^{174}Ta	91	15.9	47	0.34
	206.5	60	47	1.28
^{61}Cu	282.956	12.2	123	0.10
^{77}Kr	129.64	81	163	0.50
	146.59	37.3	163	0.23
^{82m}Rb	554.35	62.4	42	1.49
	619.11	37.98	42	0.90
	698.37	26.3	42	0.63
	776.52	84.39	42	2.01
	827.83	21	42	0.50
	1044.08	32.07	42	0.76
	1317.43	23.7	42	0.56
	1474.88	15.5	42	0.37
^{85}Y	231.7	22.8	116	0.20

^{95}Ru	336.4	70.2	28	2.51
	626.83	17.8	28	0.64
	1096.8	21	28	0.75
^{99}Rh	340.8	70	14.8	4.73
	617.8	12	14.8	0.81
	1261.2	11.1	14.8	0.75
^{121}I	212.2	84.3	21.2	3.98
^{173}Ta	63.243	12.8	13.7	0.93
	172.2	17.5	13.7	1.28
^{184}Ir	71.414	10.4	24.7	0.42
	119.79	30.8	24.7	1.25
	263.98	64.4	24.7	2.61
	390.36	26.1	24.7	1.06
	961.26	10.2	24.7	0.41

[00114] An overall quality factor ($Q_{overall}$) was calculated by using the formula:

$$Q_{overall} = Q_{production} \times Intensity\ Ratio \qquad (7)$$

[00115] For isotopes with more than one production process in one setting, the total production quality factor ($Q_{production}$) was determined as a sum of weighted averages for each production process. Results are shown in Table 6.

[00116] Also, it was noted that gamma energies that are close to 511 keV may be less effective. If the primary photon energy is close to 511 keV, then the advantages of the dual energy aspect may not be fully realized. How close the primary photon energy could be to 511 keV and still be useful as dual energy imaging was assessed by looking at water attenuation coefficients. Since the attenuation coefficient, μ, is energy dependent, gamma energies for which $\mu(E_\gamma)$ values are too close to μ(511 keV) were excluded. Table 6 shows attenuation ratio values that were calculated using the following formula:

$$\text{Attenuation Ratio} = 1 / |1-(\mu_{water}(511\ keV))/(\mu_{water}(E_\gamma))| \qquad (8)$$

[00117] Energies with attenuation ratio greater than 10 were expected to be less effective and therefore and are crossed out in Table 6. Although some gamma energies were deemed less useful, it can be seen that all 17 isotopes still remain good candidates for PET/SPECT imaging.

Table 6

Isotope	Eγ*	Q.F.	I ratio	Q.F. (overall)	μ ratio

	(keV)	(production)			
^{81}Rb	190.46	6.4	1.19	7.64	3.22
	~~446.15~~	~~6.4~~	~~0.43~~	~~2.76~~	~~18.08~~
^{123}Xe	148.9	40	1.08	43.37	2.75
	178.1	40	0.33	13.22	3.07
^{43}Sc	372.9	0.31	0.13	0.04	8.32
^{66}Ge	43.89	0.48	0.62	0.30	1.63
	108.85	0.48	0.23	0.11	2.36
	381.85	0.48	0.60	0.29	8.92
^{73}Se	67.07	35	0.54	18.73	1.96
	361.2	35	0.74	25.96	7.61
^{75}Br	286.5	6	0.62	3.70	4.88
^{90}Mo	122.37	4.6	1.28	5.89	2.49
	257.34	4.6	1.56	7.18	4.25
^{174}Ta	91	51	0.34	17.25	2.20
	206.5	51	1.28	65.11	3.43
^{61}Cu	282.956	3.1	0.10	0.31	4.81
^{77}Kr	129.64	15	0.50	7.45	2.56
	146.59	15	0.23	3.43	2.73
^{82m}Rb	~~554.35~~	~~25~~	~~1.49~~	~~37.14~~	~~28.26~~
	~~619.11~~	~~25~~	~~0.90~~	~~22.61~~	~~11.55~~
	698.37	25	0.63	15.65	6.82
	776.52	25	2.01	50.23	4.91
	827.83	25	0.50	12.50	4.17
	1044.08	25	0.76	19.09	2.59
	1317.43	25	0.56	14.11	1.79
	1474.88	25	0.37	9.23	1.53
^{85}Y	231.7	17	0.20	3.34	3.80
^{95}Ru	336.4	1.1	2.51	2.76	6.45
	~~626.83~~	~~1.1~~	~~0.64~~	~~0.70~~	~~10.81~~
	~~1096.8~~	~~1.1~~	~~0.75~~	~~0.83~~	~~2.38~~
^{99}Rh	340.8	100	4.73	472.97	6.64
	~~617.8~~	~~100~~	~~0.81~~	~~81.08~~	~~11.70~~
	1261.2	100	0.75	75.00	1.91
^{121}I	212.2	3.5	3.98	13.92	3.50
^{173}Ta	63.243	4.3	0.93	4.02	1.91
	172.2	4.3	1.28	5.49	3.00
^{184}Ir	71.414	32	0.42	13.47	2.01
	119.79	32	1.25	39.90	2.47
	263.98	32	2.61	83.43	4.38
	390.36	32	1.06	33.81	9.55
	961.26	32	0.41	13.21	3.02

[00118] From Table 6, it can be seen that ^{123}Xe, ^{73}Se, ^{174}Ta, ^{99}Rh and ^{184}Ir are strong candidates as combined PET/SPECT isotopes.

[00119] The ^{123}Xe isotope ($T_{1/2}$= 2.08 hours) can be produced by $^{127}I(p,5n)$ ^{123}Xe reaction in which protons will be bombarded on a ^{127}I target (100% natural abundance). The decay product ^{123}I is a commonly used isotope for thyroid cancer diagnosis. The threshold energy of protons for this reaction is 37.1 MeV. Figure 7 shows the neutron cross section (a measure of production rate) plotted against proton energy. As shown, it is reasonable to assume that sufficient amounts of ^{123}Xe can be produced with 55-60 MeV proton beam currents of several micro amperes.

[00120] About 22% of the decay events of ^{123}Xe are by the emission of positrons populating the 149 keV and 178 keV levels in ^{123}I which in turn emit photons of corresponding energies. Thus, almost every emitted positron is accompanied by a gamma photon having an energy of either about 178 keV or about 149 keV. Accordingly, ^{123}Xe may improve the imaging compared to single photon imaging using the 142 keV photon of ^{99m}Tc, typically used in current SPECT imaging.

[00121] It is also encouraging that xenon is administered to patients for xenon enhanced CT as it propagates in the human body. This technique is advocated for brain imaging as it is not limited by the blood-brain barrier (see for example N. Miyazawa, M. Uchida, A. Fukamachi, I. Fukasawa, H. Sasaki, and H. Nukui, American Journal of Neuroradiology, (1999), vol. 20, p. 1858-1862).

[00122] Also, the decay product ^{123}I is a commonly employed SPECT isotope for thyroid imaging.

[00123] Thus, ^{123}Xe isotope has a great promise to be useful for whole body PET/SPECT imaging.

[00124] The ^{73}Se isotope ($T_{1/2}$=7.5 hrs) can be produced via the $^{75}As(p,3n)$ ^{73}Se reaction, where ^{75}As (which has a high natural abundance) is bombarded with proton beams. The threshold for this reaction is 22.0 MeV, with a maximum at proton energies of about 34 MeV (see Figure 8).

[00125] One may also consider the $^{76}Se(p,2n)$ and $^{77}Se(p,3n)$ reactions which are of high cross sections at about 23 MeV and above 30 MeV, respectively. The natural abundances of these isotopes ^{76}Se (9.4%) and ^{77}Se(7.6%) are relatively

small, but still higher than that of ^{18}O (0.2%), the radioisotope used in the production of FDG. One can thus expect a factor of 30 higher production rates with solid samples, which are easier to handle than the liquid water targets enriched in ^{18}O used in the production of FDG.

[00126] In the decay of ^{73}Se, the positron emission is accompanied by 67 keV and 361 keV photons. Thus, it provides a very interesting contrast of very low energy (67 keV), and somewhat high energy (361keV) photons in addition to the 511 keV photons which result from the positron annihilation. Accordingly, ^{73}Se could prove very useful in identifying soft tissue, dense material and bones distinctly.

[00127] The ^{73}Se isotope looks promising for use in measuring and assessing the bile acid turnover in the intestines, based on the current use of SeHCAT (selenium homocholic acid taurine or tauroselcholic acid), a radiopharmaceutical incorporating the gamma emitter ^{75}Se. Also, the National Oncology Research Institute is carrying out extensive research on selenium as a selective chemotherapeutic agent, indicating that administering selenium to humans or animals has therapeutic applications. Thus, selenium isotopes appear to be good candidates for diagnostic purposes.

[00128] The ^{75}Br isotope ($T_{1/2}$ = 96.7 minutes) emits 286 keV photons in addition to positrons.

[00129] Valette and coworkers produced Metabromobenzylguanidine (MBBG), a bromine compound as a PET radiotracer (H. Valette, C. Loc'h, K. Mardon, B. Bendriem, P. Merlet, C. Fuseau, S. Sabry, D. Raffel, B. Maziere, and A. Syrota, The Journal of Nuclear Medicine, Vol. 34 (1993) p. 1739-1744.). Bromine belongs to the same group as fluorine, the radioisotope used in FDG for PET imaging. Therefore, as fluorine and bromine belong to the same group in periodic table, they can be substituted each other. Also, as MBBG does to heart imaging what FDG does to metabolically active tissues, it is conceivable that MBBG can be substituted employed for heart imaging, with the added advantage of the dual PET/SPECT imaging described above, as opposed to the typical PET imaging of FDG.

[00130] The systems, processes and methods of the described embodiments are capable of being implemented in a computer program product comprising a non-

transitory computer readable medium that stores computer usable instructions for one or more processors that cause the one or more processors to operate in a specific and predefined manner to perform the functions described herein. The medium may be provided in various forms, including as volatile or non-volatile memory provided on optical, magnetic or electronic storage media.

[00131] While the above description describes features of example embodiments, it will be appreciated that some features and/or functions of the described embodiments are susceptible to modification without departing from the spirit and principles of operation of the described embodiments. Accordingly, what has been described above is intended to be illustrative of the claimed concept and non-limiting. It will be understood by persons skilled in the art that variations are possible in variant implementations and embodiments.

CLAIMS:

1. A method of determining an approximate location of a radionuclide at a time of radioactive decay of the radionuclide, the method comprising:

a) providing a plurality of photon detectors directed towards a target region;

b) introducing into the target region the radionuclide that, at the time of its radioactive decay, emits a positron and a primary photon;

c) detecting the primary photon at a first one of the plurality of photon detectors and detecting at least one secondary photon emitted from an annihilation of the positron at at least a second one of the plurality of photon detectors; and

d) determining the approximate location of the radionuclide at the time of its radioactive decay based on a location of the first one of the plurality of photon detectors, a location of the second one of the plurality of photon detectors, and a presumed common point of origin of the detected primary photon and the detected at least one secondary photon.

2. The method of claim 1, wherein the primary photon is emitted from a daughter product of the radionuclide following the emission of the positron.

3. The method of any one of claims 1 to 2, wherein the plurality of photon detectors is capable of characterizing a detected photon as either primary or secondary.

4. The method of claim 3, wherein the primary photon has a primary expected energy, the at least one secondary photon has a secondary expected energy, and wherein the characterizing is based on a comparison of a detected energy of the detected photon and at least one of the primary and secondary expected energies.

5. The method of any one of claims 1 to 4, wherein the determining is further based on a time of detection of the primary photon and a time of detection of each of the at least one secondary photon.

6. The method of any one of claims 1 to 5, wherein the detecting at least one secondary photon comprises detecting two secondary photons.

7. The method of claim 6, wherein the approximate location of the radionuclide at the time of its radioactive decay is determined based on a selected two of the three detected photons.

8. The method of claim 6, wherein the approximate location of the radionuclide at the time of its radioactive decay is determined based on a selected one of the three detected photons.

9. The method of any one of claims 1 to 8, wherein the detecting of the primary photon and the at least one secondary photon is performed during a predetermined time interval.

10. The method of any one of claims 1 to 9, wherein the plurality of photon detectors comprises a ring of photon detectors disposed about the target region.

11. The method of any one of claims 1 to 10, wherein the introducing comprises introducing a molecule or compound tagged with a plurality of radionuclides into the target region.

12. The method of claim 11, further comprising

i) repeating the detecting over a plurality of predetermined time intervals, and,

ii) for substantially each predetermined time interval in the plurality of predetermined time intervals during which one of the plurality of radionuclides undergoes radioactive decay, determining the approximate location of that radionuclide at the time of its radioactive decay based on a presumed common point of origin of photons detected during that predetermined time interval.

13. The method of any one of claims 11 to 12, further comprising determining a volumetric reconstruction of a concentration of the plurality of radionuclides within the object based on a statistical reconstruction of the determined approximate locations of substantially each of the plurality of radionuclides.

14. The method of any one of claims 1 to 13, wherein the radionuclide is ^{123}Xe, ^{73}Se, ^{75}Br, ^{174}Ta, ^{99}Rh, or ^{184}Ir.

15. The method of claim 14, wherein the radionuclide is ^{123}Xe.

16. The method of claim 14, wherein the radionuclide is ^{73}Se.

17. A system for determining an approximate location of a radionuclide that, at the time of its radioactive decay, emits a positron and a primary photon, the system comprising:

a) a plurality of photon detectors directed towards a target region, the plurality of photon detectors capable of detecting the primary photon at a first one of the plurality of photon detectors and detecting at least one secondary photon emitted from an interaction of the positron and an electron at least a second one of the plurality of photon detectors; and

b) a computing device capable of determining the approximate location of the radionuclide at the time of its radioactive decay based on a location of the first one of the plurality of photon detectors, a location of the second one of the plurality of photon detectors, and a presumed common point of origin of the detected primary photon and the detected at least one secondary photon.

18. A method of localizing a radioisotope within a target region at a time of radioactive decay of the radioisotope, the method comprising:

a) providing at least one photon detector directed towards the target region;

b) introducing the radioisotope into the target region, the radioisotope comprising a radioisotope that, at the time of radioactive decay, emits a positron and at least one primary photon;

c) detecting the at least one primary photon and at least one secondary photon emitted from an interaction of the positron and an electron using the at least one photon detector; and

d) localizing the radioisotope based on the detected at least one primary photon and the detected at least one secondary photon.

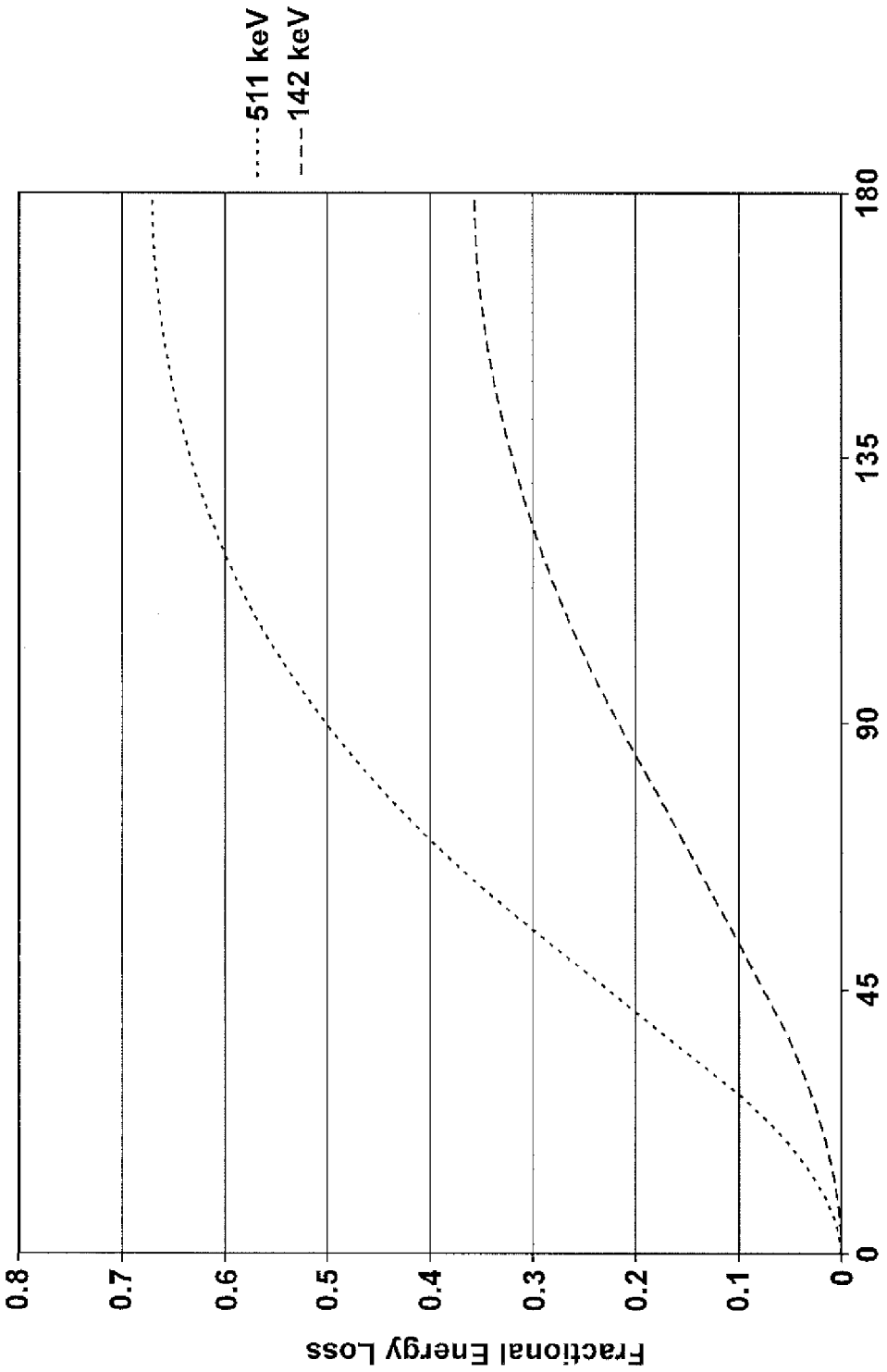
511 keV
142 keV
Fractional Energy Loss
0.8
0.7
0.6
0.5
0.4
0.3
0.2
0.1
0
0
45
90
135
180
Scattering Angle

FIG. 1

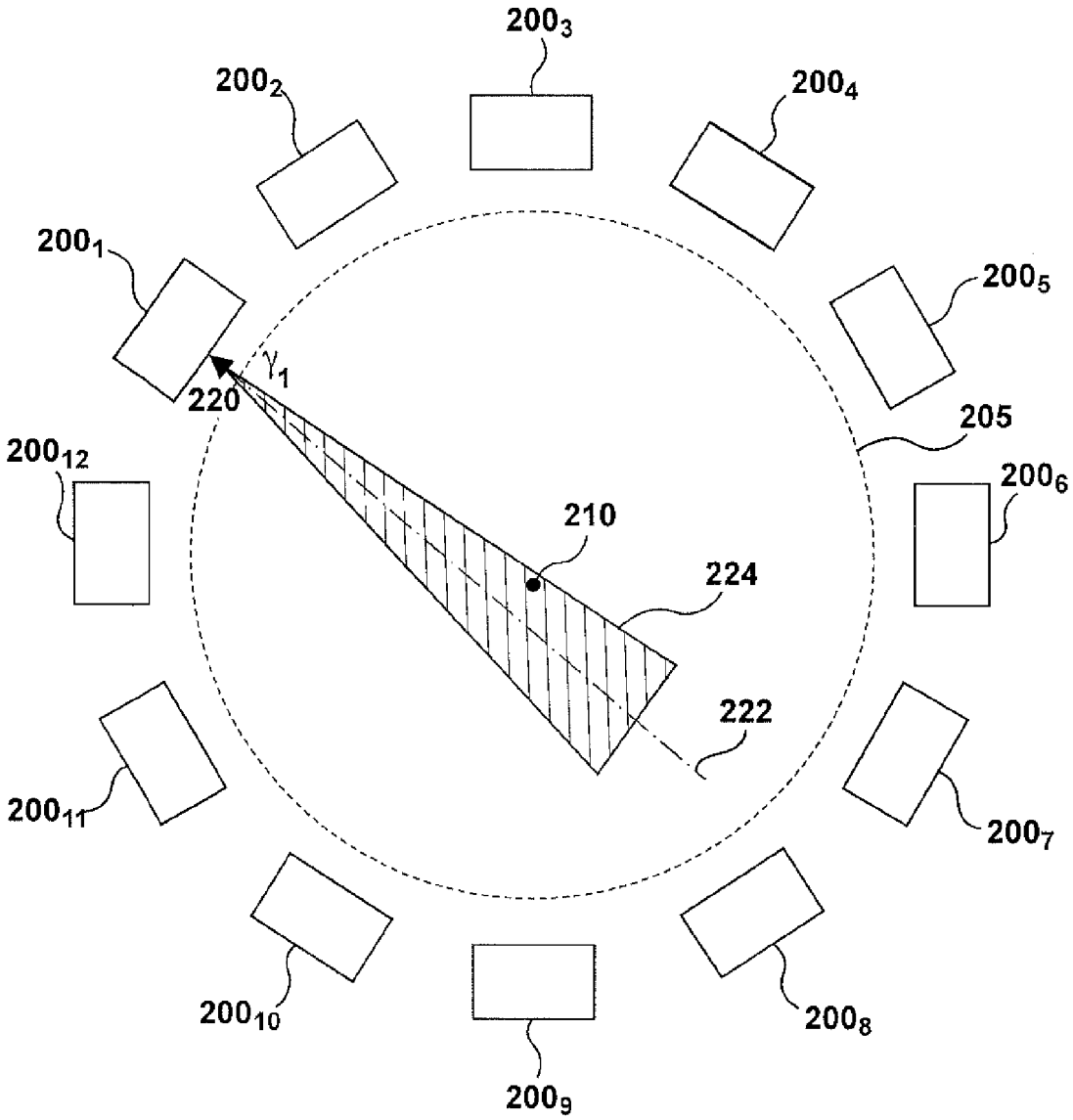
200_3
200_2
200_4
200_1
200_5
γ_1
220
205
200_{12}
200_6
210
224
222
200_{11}
200_7
200_{10}
200_8
200_9

FIG. 2

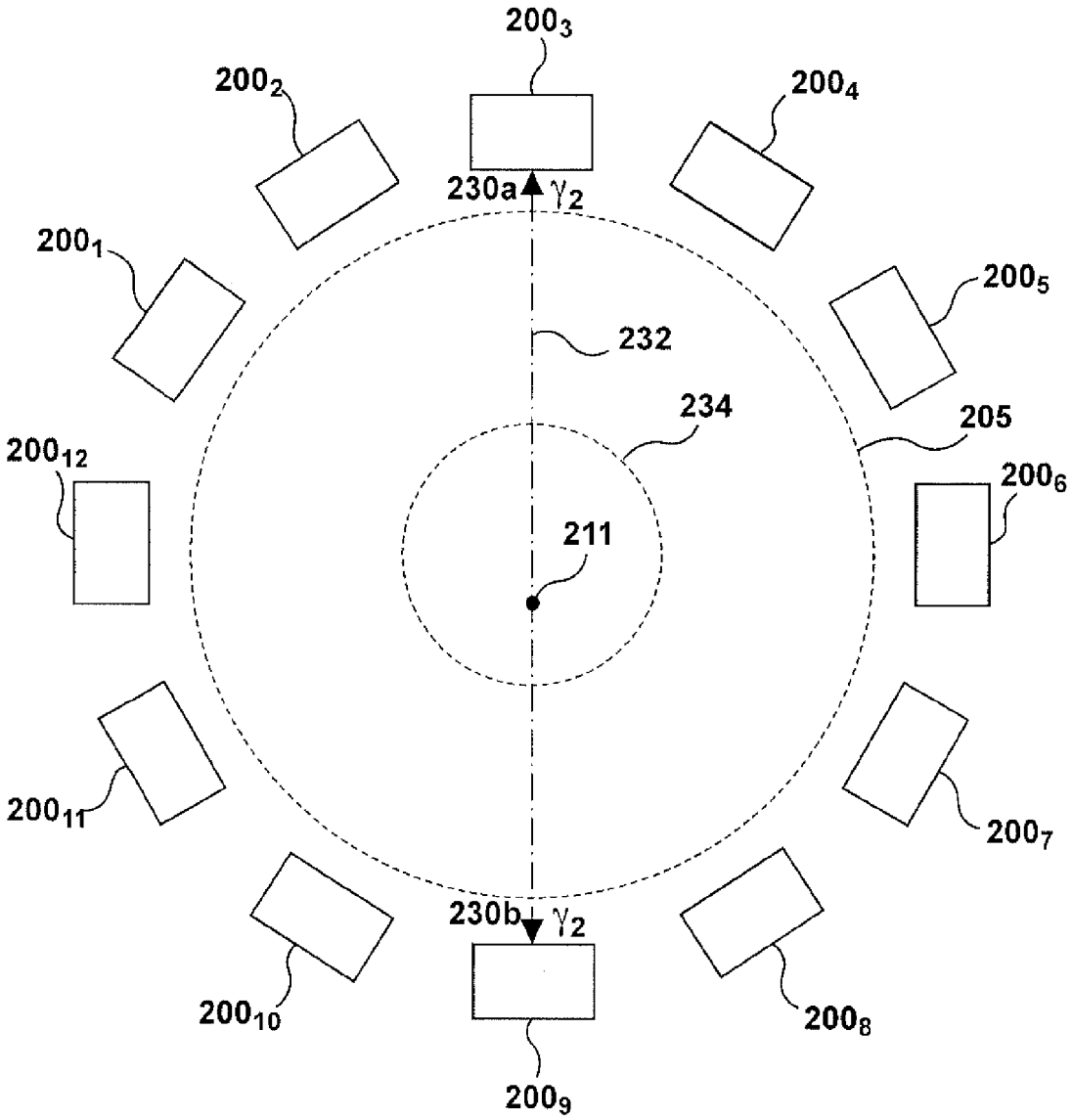
200_3
200_2
200_4
230a
γ_2
200_1
200_5
232
234
205
200_{12}
200_6
211
200_{11}
200_7
230b
γ_2
200_{10}
200_8
200_9

FIG. 3

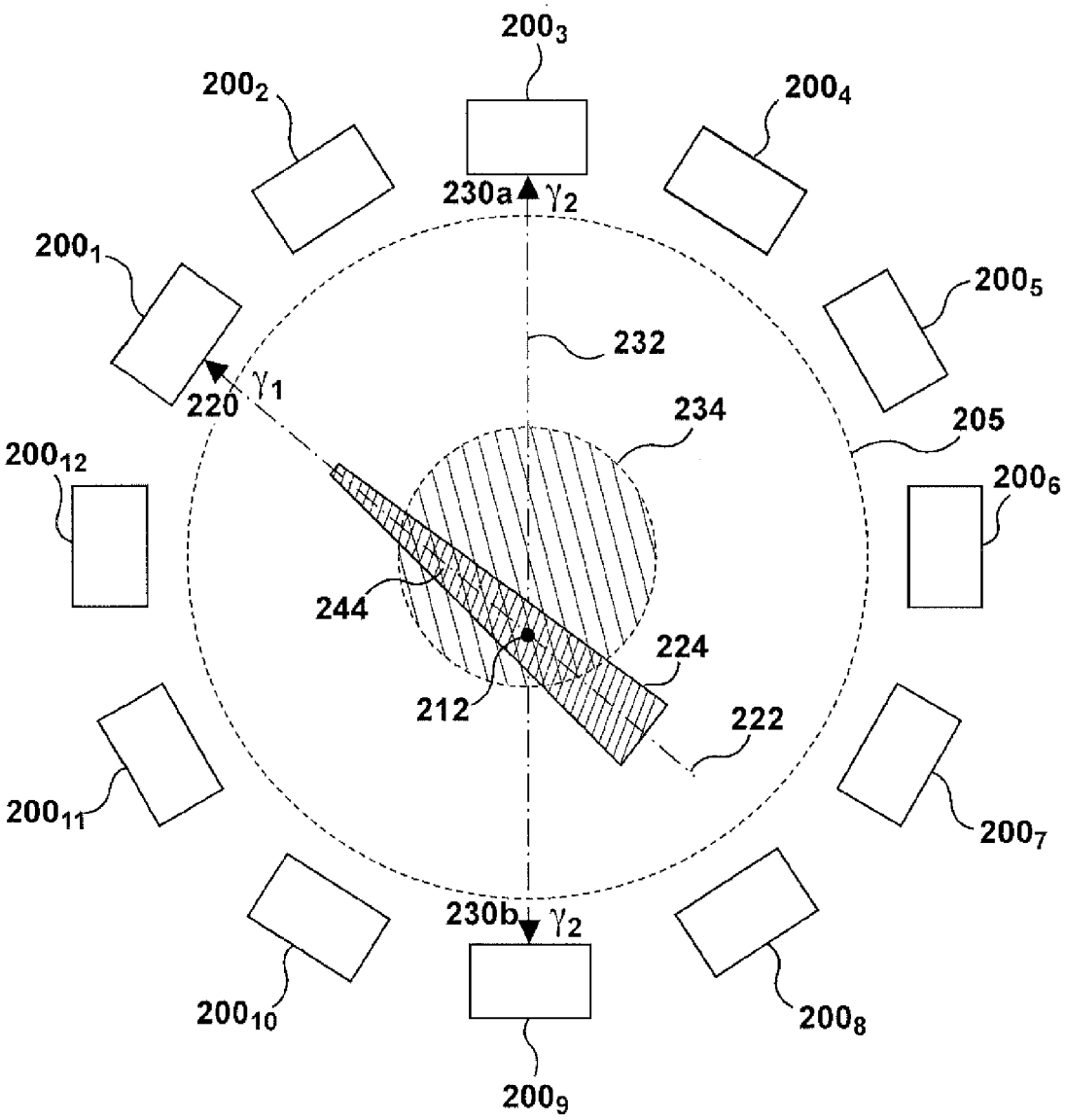
200_3
200_2
200_4
230a
γ_2
200_1
200_5
232
220
γ_1
234
205
200_{12}
200_6
244
224
212
222
200_{11}
200_7
230b
γ_2
200_{10}
200_8
200_9

FIG. 4

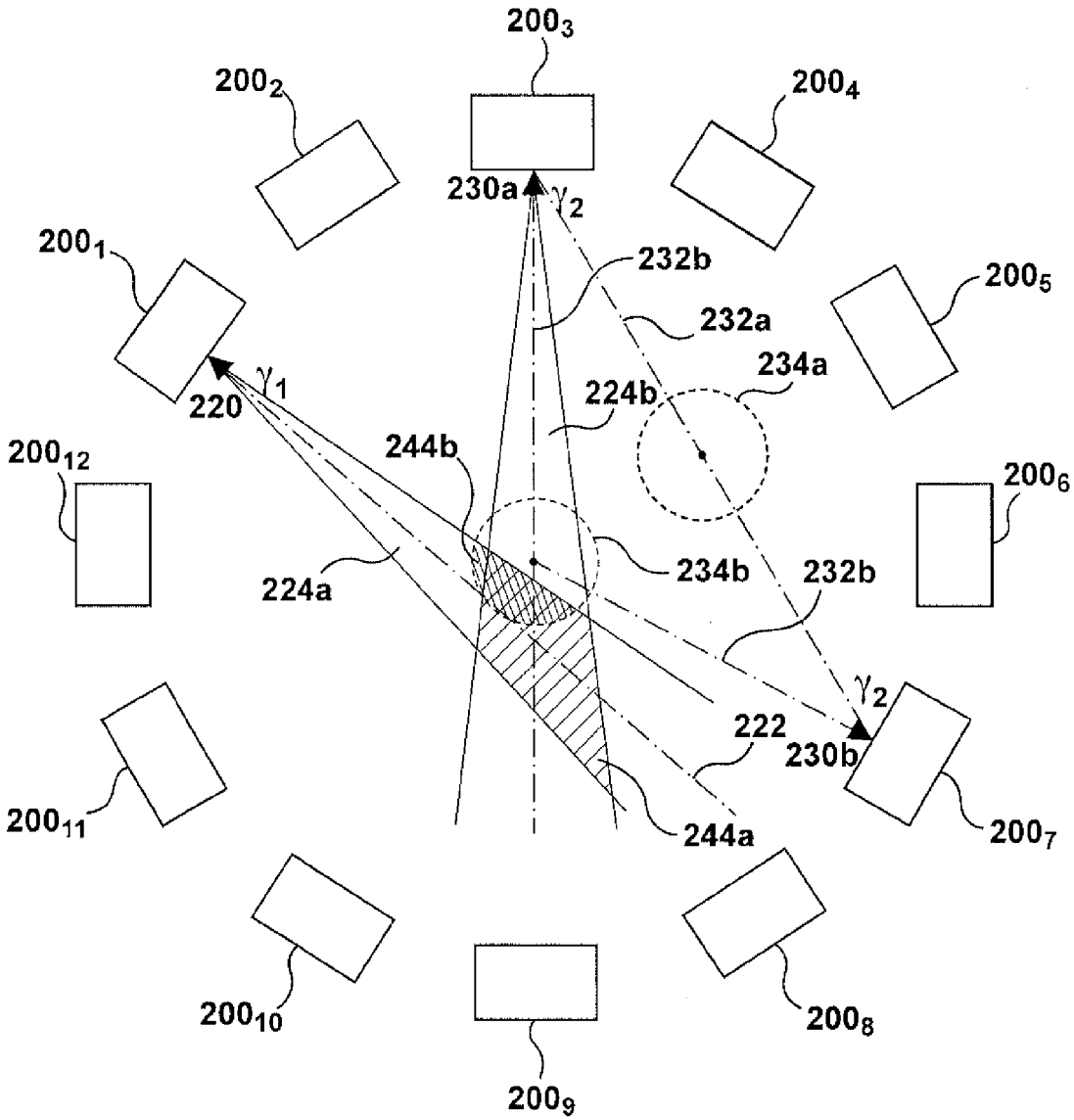
200_3
200_2
200_4
230a
γ_2
200_1
232b
200_5
232a
234a
γ_1
220
224b
244b
200_{12}
200_6
234b
232b
224a
γ_2
222
230b
200_{11}
244a
200_7
200_{10}
200_8
200_9

FIG. 5

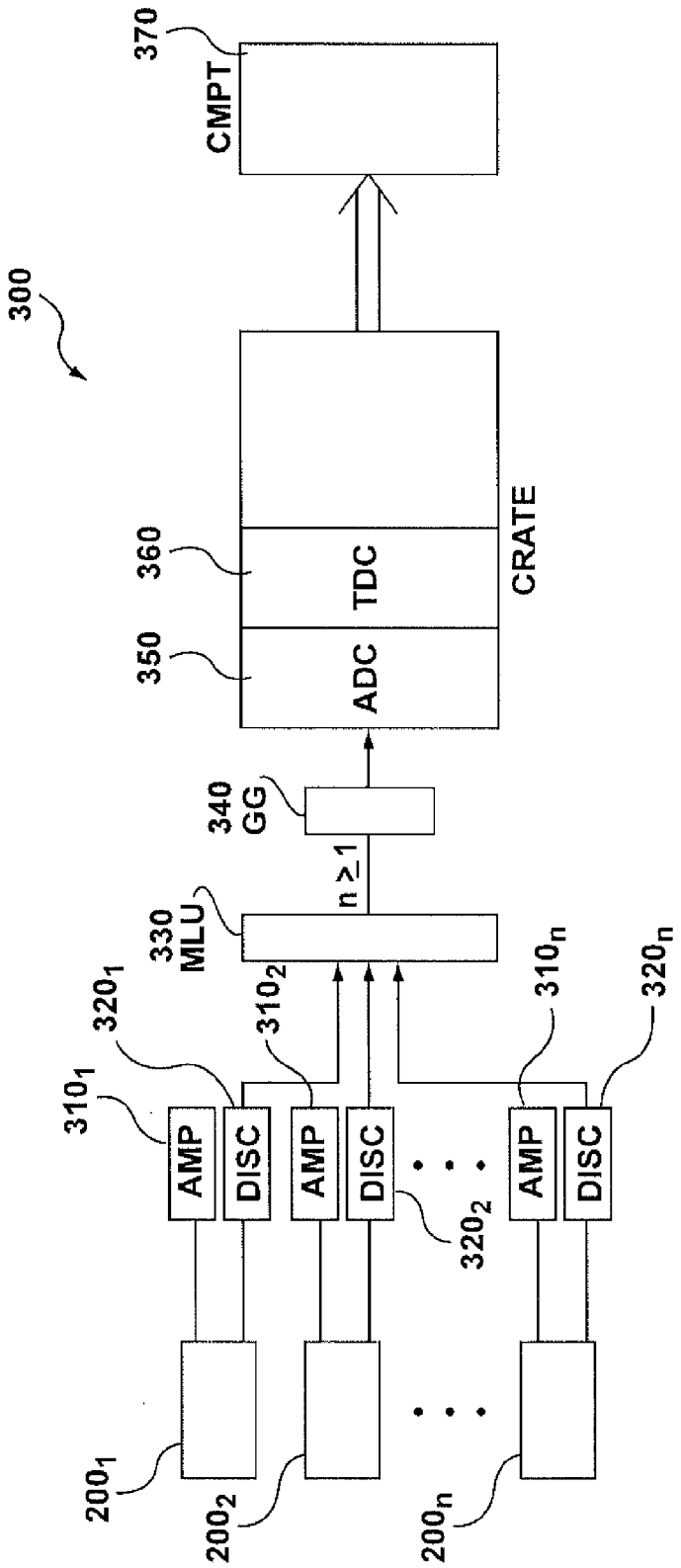
300
370
CMPT
360
TDC
350
ADC
CRATE
340
GG
n ≥ 1
330
MLU
320_1
310_1
310_2
320_2
310_n
320_n
AMP
DISC
200_1
200_2
200_n

FIG. 6

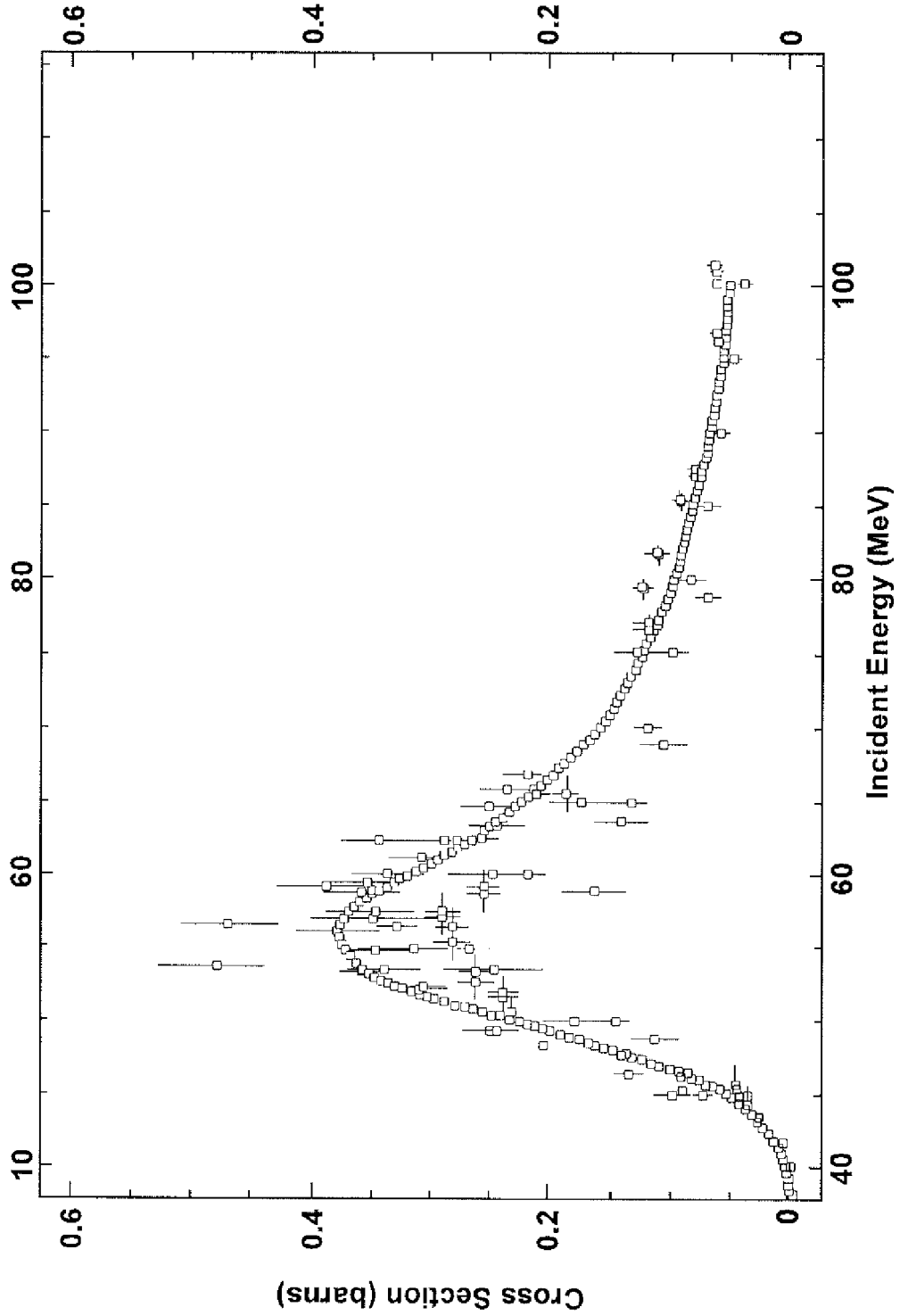
Cross Section (barns)
0
0.2
0.4
0.6
10
40
60
80
100
Incident Energy (MeV)

FIG. 7

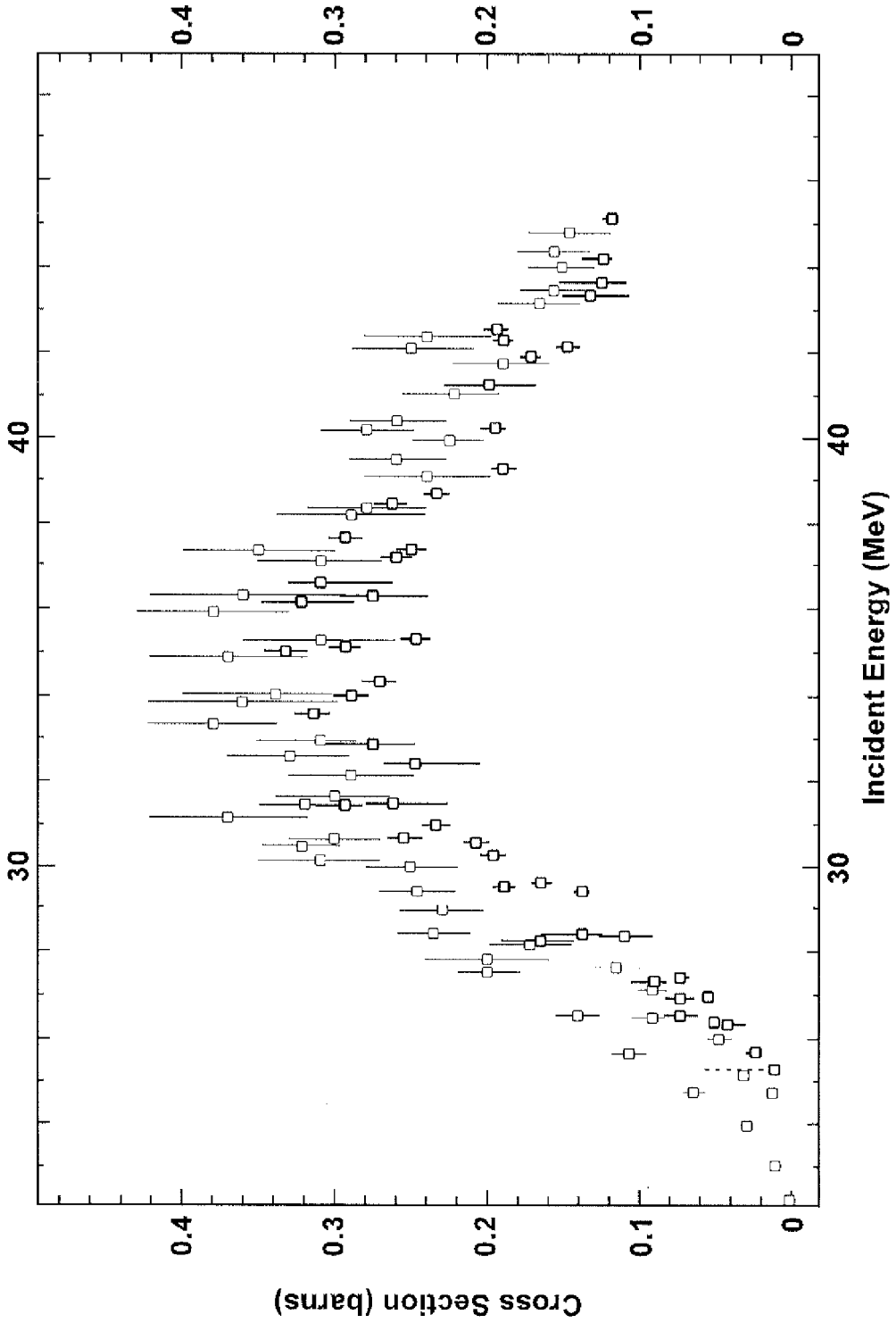

FIG. 8

INTERNATIONAL SEARCH REPORT

International application No.
PCT/CA2013/050556

A. CLASSIFICATION OF SUBJECT MATTER

IPC: ***G01T 1/164*** (2006.01) , ***G01T 1/169*** (2006.01)

According to International Patent Classification (IPC) or to both national classification and IPC

B. FIELDS SEARCHED

Minimum documentation searched (classification system followed by classification symbols)

IPC: ***G01T 1/164*** (2006.01) , ***G01T 1/169*** (2006.01)

Documentation searched other than minimum documentation to the extent that such documents are included in the fields searched

Electronic database(s) consulted during the international search (name of database(s) and, where practicable, search terms used)

TotalPatent, Canadian Patent Database (Intellect), and World Wide Web. Keywords: primary, secondary, photon, positron, scatter, energy, position/localize/location, daughter product, coincident, event, decay, xenon/Xe, selenium/Se, neutrino, nucleus, detect, imag*, emit,

C. DOCUMENTS CONSIDERED TO BE RELEVANT

Category*	Citation of document, with indication, where appropriate, of the relevant passages	Relevant to claim No.
X Y	US 7 888 651 (CHINN et al.) 15 February 2011 (15-02-2011) *See: abstract; col. 1, l. 33-41; col. 2, l. 52-65; col. 3, l. 7-20; col. 3, l. 62 - col. 4, l. 39; col. 4, l. 64 - col. 5, l. 9; col. 7, l. 35-45; col. 8, l. 60 - col. 9, l. 5; and fig. 12C.	1-13, 17 and 18 14-16
Y	YAMAMOTO et al. "Positron Emission Tomography for Measurement of Regional Cerebral Blood Flow", Advances in Neurology, Vol. 30, pgs. 41-53, 1981 *See: pg. 44, right-hand-column, 2nd para.	14-16
A	EP 2 360 493 (EIGEN) 24 August 2011 (24-08-2011) *See: entire document	1-18

[ ] Further documents are listed in the continuation of Box C.

[X] See patent family annex.

* Special categories of cited documents :

"A" document defining the general state of the art which is not considered to be of particular relevance

"E" earlier application or patent but published on or after the international filing date

"L" document which may throw doubts on priority claim(s) or which is cited to establish the publication date of another citation or other special reason (as specified)

"O" document referring to an oral disclosure, use, exhibition or other means

"P" document published prior to the international filing date but later than the priority date claimed

"T" later document published after the international filing date or priority date and not in conflict with the application but cited to understand the principle or theory underlying the invention

"X" document of particular relevance; the claimed invention cannot be considered novel or cannot be considered to involve an inventive step when the document is taken alone

"Y" document of particular relevance; the claimed invention cannot be considered to involve an inventive step when the document is combined with one or more other such documents, such combination being obvious to a person skilled in the art

"&" document member of the same patent family

Date of the actual completion of the international search	Date of mailing of the international search report
15 August 2013 (15-08-2013)	07 November 2013 (07-11-2013)

Name and mailing address of the ISA/CA	Authorized officer
Canadian Intellectual Property Office Place du Portage I, C114 - 1st Floor, Box PCT 50 Victoria Street Gatineau, Quebec K1A 0C9 Facsimile No.: 001-819-953-2476	Bryon Braymore (819) 934-6753

INTERNATIONAL SEARCH REPORT
Information on patent family members

International application No.
PCT/CA2013/050556

Patent Document Cited in Search Report	Publication Date	Patent Family Member(s)	Publication Date
US7888651B2	15 February 2011 (15-02-2011)	US2009078876A1	26 March 2009 (26-03-2009)
		US2010148075A1	17 June 2010 (17-06-2010)
		US7968850B2	28 June 2011 (28-06-2011)
		US2009072156A1	19 March 2009 (19-03-2009)
		US8183531B2	22 May 2012 (22-05-2012)
EP2360493A1	24 August 2011 (24-08-2011)	EP2360493A1	24 August 2011 (24-08-2011)
		US2011198504A1	18 August 2011 (18-08-2011)